Published in final edited form as:
Crit Rev Biomed Eng. 2011 ; 39(5): 397–433.

Nitric Oxide Signaling in the Microcirculation

Donald G. Buerk, **Kenneth A. Barbee**, and **Dov Jaron***
School of Biomedical Engineering, Science, and Health Systems, Drexel University, Philadelphia, Pennsylvania

Abstract

Several apparent paradoxes are evident when one compares mathematical predictions from models of nitric oxide (NO) diffusion and convection in vasculature structures with experimental measurements of NO (or related metabolites) in animal and human studies. Values for NO predicted from mathematical models are generally much lower than in vivo NO values reported in the literature for experiments, specifically with NO microelectrodes positioned at perivascular locations next to different sizes of blood vessels in the microcirculation and NO electrodes inserted into a wide range of tissues supplied by the microcirculation of each specific organ system under investigation. There continues to be uncertainty about the roles of NO scavenging by hemoglobin versus a storage function that may conserve NO, and other signaling targets for NO need to be considered. This review describes model predictions and relevant experimental data with respect to several signaling pathways in the microcirculation that involve NO.

Keywords

calcium; endothelium; mathematical models; microcirculation; nitric oxide; shear stress

I. INTRODUCTION

Murad and Barber[1] hypothesize that nitric oxide (NO) must have evolved as one of the earliest signaling molecules in primitive organisms, preceding the presence of O_2 in the atmosphere and the subsequent evolution of heme-containing proteins. In the 30 years since NO was identified as the endothelium-derived relaxing factor[2,3] produced by NO synthases (NOS; isoforms include endothelial NOS [eNOS], neuronal NOS [nNOS], immunologic NOS [iNOS], and possibly mitochondrial NOS), NO now is recognized to be a ubiquitous signaling molecule with a multitude of diverse biological actions. Significant advances in understanding the complex chemistry of NO have been made. Signaling involves direct reactions between NO and a molecular target or can occur through indirect reactions of secondary reactive nitrogen species with signaling targets.[4] However, contradictory results are reported in the literature, especially with regard to pathophysiologic disturbances in NO signaling. There continues to be debate about what levels of NO are involved, whether there is a clearly defined threshold at which NO crosses from being beneficial to being destructive, and whether there are mechanisms to conserve NO scavenged by hemoglobin (Hb) in the bloodstream to increase downstream NO bioavailability to the vascular wall.

Thomas et al.[5] note that the biological function of NO seems to depend greatly on concentration, although the time course of exposure to NO also may be critical. Many

*Address all correspondence to: Dov Jaron, PhD, School of Biomedical Engineering, Science, and Health Systems, Drexel University, 3141 Market St., Philadelphia, PA 19104; dov.jaron@drexel.edu..

studies cited in their review were conducted using NO donors to produce well-controlled NO concentrations. They postulate that there are 5 distinct NO concentration ranges associated with different molecular targets for NO, and they review the evidence for different processes that occur for these targets. The lowest NO range (<30 nM) is associated with cyclic guanosine monophosphate (cGMP)–mediated processes. The next range (30–100 nM) involves phosphorylation of protein Akt. Stabilization of hypoxia-inducible factor-1α is proposed to occur in the next range (100–300 nM). NO is believed to play a protective role when its concentration is within these 3 ranges. At NO concentrations greater than 400 nM, p53 phosphorylation is induced, and at NO >1 μM, nitrosative stress will occur. Cytotoxic events, such as arrest of the cell cycle, cell senescence, or apoptosis, can occur at these high NO concentrations. However, Hall and Garthwaite[6] suggest that the chemical and biological reactivity of NO that has been studied using very high NO concentrations is of doubtful physiological relevance. It is their view that the normal physiologic concentration for NO should be very low, approximately 100 pM or even lower.

A computer simulation for the chemistry of reactive nitrogen species by Lancaster[7] suggests that, under physiologically relevant conditions in the presence of carbon dioxide (CO_2), nitrosation and nitration are relatively minor reactions, and that mostly oxidative reactions are predicted to occur, primarily through the oxidizing species carbonate ion (CO_3^-), nitrogen dioxide (NO_2), and peroxynitrite ($ONOO^-$) that is generated by the rapid reaction of NO with superoxide (O_2^-). Deficiencies in *L*-arginine or tetrahydropterin (BH_4) availability have been linked to increased generation of O_2^- by NOS (uncoupled NOS) with increased incidence of cardiovascular diseases (see reviews[8–10]). Also, there is evidence that the enzyme arginase, which competes for *L*-arginine as a substrate,[11], is upregulated as blood vessels age and impairs endothelial cell (EC) function.[12,13] Inhibitors of arginase can restore endothelial function and vascular compliance in old rats[14] Asymmetric dimethylarginine (ADMA), an analogue of *L*-arginine, may directly inhibit eNOS.[15] Elevated ADMA levels in blood plasma are thought to be a risk factor in hypercholesterolemia, diabetes mellitus, hypertension, chronic heart failure, coronary artery disease, erectile dysfunction, and other cardiovascular diseases.[16–18]

In this review, we will survey both theoretical and experimental studies that are relevant to understanding how NO signaling affects the mammalian microcirculation. This review will focus only on mathematical models that are particularly relevant to the microcirculation and will not consider models that have been developed for other physiologic systems. Effects of oxidative stress with reactive oxygen species and a few pathologic alterations in NO signaling will be discussed briefly, but further details are left to other reviews in this issue.

II. CALCIUM, ION CHANNELS, SHEAR STRESS, AND NITRIC OXIDE PRODUCTION BY ENDOTHELIAL CELLS

Modeling at the cellular level can prove to be useful in understanding normal microcirculatory function as well as to provide insight into pathophysiologic processes that lead to vascular disease. Although exact mechanisms by which ECs sense blood flow and propagate signals that control the microcirculation are not fully understood, changes in Ca^{2+} and electronic transmission of membrane potential changes (V_m) seem to play major roles, especially for acute responses to changes in flow. More prolonged activation of eNOS via phosphorylation has also been demonstrated in response to shear stress.

Many candidates for wall shear stress (WSS) sensors and possible mechanisms by which ECs sense changes in blood flow have been proposed (see review[19]). Fluid flowing over the endothelium may directly deform molecular structures on the cell surface, and the stresses transmitted throughout the cell via cytoskeletal linkages or the plasma membrane potentially

can affect molecular structures capable of transducing the stress signal. Cell surface structures reported to be involved in flow sensing include the glycocalyx, plasma membrane ion channels, cell surface receptors, and caveolae. Important signaling sites located away from the exposed surface of the cells include focal adhesion complexes and cell-cell adhesion complexes. Finally, because the mechanical stimulus is caused by fluid flow, changes in stress are inextricably coupled to changes in transport processes at the cell surface. Changes in convective transport affect the delivery of blood-borne agonists and the removal of secreted factors that can play a role in the overall response of the cell.

An early response to flow typically observed in ECs is a rapid transient increase in $[Ca^{2+}]_i$ that depends on the magnitude of shear stress.[20,21] Typical $[Ca^{2+}]_i$ responses following step changes in shear stress were recently reported for bovine aortic ECs by Hong et al.[22] Fluorescence imaging shows a synchronous response with higher average peak amplitude at higher shear stresses (Fig. 1A), with similar rapid time courses for individual measurements (Fig. 1B). In contrast, heterogeneous responses with multiple peaks were observed with rat adrenomedullary ECs derived from capillary endothelium (Fig. 1C). Also, Ca^{2+} oscillations in individual ECs that did not propagate to neighboring ECs frequently were observed. Some ECs had Ca^{2+} responses that were delayed in time after initiation of shear stress (Fig. 1D). Though the time to peak was tightly grouped at around 15 s for BAECs, there was a wide distribution of peak times for the rat adrenomedullary ECs over a 5-min period after the change in WSS. These findings highlight the heterogeneity of endothelial cells both regionally (microvascular vs. large vessel) and among individual cells.

An in vitro study with isolated pig femoral arteries treated with enzymes to degrade specific components of EC glycocalyx reported that hyaluronic acid is involved in sensing WSS and NO production because removal decreased vasodilation and nitrite production.[23] Other components of EC glycocalyx (heparin sulfate and sialic acid) do not seem to be involved in WSS sensing, but have an effect on NO bioavailability because they seem to be associated with modulating O_2^- generation through the presence of extracellular superoxide dismutase.

Nauli et al.[24] reported that cilia on the apical membrane of ECs and polycystin-1, a cilia-specific protein, act as fluid shear sensors based on optical measurements of $[Ca^{2+}]_i$ and NO in cultured mouse ECs. Mutant ECs from mice lacking specific genes that regulate cilia and polycystin-1 did not respond to shear stress. Polycystin-1 modulates polycystin-2, a protein cation channel that belongs to a superfamily of transient receptor potential (TRP) ion channels, and there is evidence that this ion channel has a specific shear-sensing role in ECs.[25] The role of TRP vanilla type 4 (TRPV4) channels has been studied in small resistance arteries from the mesentery of wild type and TRPV4-null mice.[26] An agonist to the TVRP4 channel caused rapid increases in EC $[Ca^{2+}]_i$ in blood vessels from wild-type but not TVRP4-null mice. The Ca^{2+} response to WSS could be blocked with pharmacologic inhibitors of TRPV4 channels and by gene-specific small interfering RNA.

eNOS is found in plasma membrane invagi-nations called *caveolae*, where association with the protein caveolin-1 inhibits its activity. Because of the structure and location of caveolae on the flow-contacting surface of ECs, they have been proposed as a mechanosensory structure.[27] In an in situ flow model, Rizzo et al.[27] showed shear stress–induced release of eNOS from its inhibitory association with cav-1 and increased association with calmodulin.

Shear stress has been shown to activate eNOS via Akt/protein kinase (PK) B–dependent phosphorylation of Ser1177.[28] Several mechanisms for initiating this pathway have been proposed. Activation of the vascular endothelial growth factor receptor independent of ligand binding caused Akt and eNOS activation, providing an example of a cell surface molecule acting as a mechanochemical transducer.[29] The platelet EC adhesion molecule

(PECAM), found primarily at EC junctions, also has been implicated in the shear stress response. Flow-induced phosphorylation of PECAM caused association of PECAM with eNOS and activation of eNOS via the Akt pathway.[30] However, PECAM phosphorylation could be blocked by tyrosine kinase inhibition, so it seems that PECAM itself is not the stress sensor. Finally, α_1 integrin also has been shown to modulate shear stress–dependent phosphorylation of eNOS. In mouse mesenteric resistance arteries, both anti-α_1 blocking antibodies and genetic deficiency in α_1-integrin ($\alpha_1(-/-)$) inhibited flow-induced vasodilation by blocking eNOS phosphorylation via the Akt-eNOS pathway.[31]

It is important to note that there are conflicting reports about the relative importance of Ca-dependent and -independent pathways for eNOS activation and NO production. These discrepancies may be because of the use of different species or vascular beds. Significant differences between the structure and gene expression profiles of ECs in culture and those of ECs in vivo, or from isolated vessel preparations, are to be expected. It is clear that not only the level of expression of relevant signaling molecules but also their spatial arrangement within the EC can modulate the mechanism of response[32] as well as the manner in which mechanical forces are distributed throughout the EC.[33] Hopefully, the development of techniques to make measurements with better temporal and spatial resolution in combination with mathematical modeling of the complex interplay of mechanics, transport, and biochemical reactions will help resolve these issues.

II.A. Modeling Ca^{2+} Kinetics in Endothelial Cells

Normally, active transport maintains free Ca^{2+} in EC cytosol at a very low concentration. This is accomplished in part by storing Ca^{2+} in the endoplasmic reticulum. In response to mechanical stimuli or local chemical stimulation by agonists, $[Ca^{2+}]_i$ can be increased by Ca^{2+} release from ER by inositol triphosphate (IP_3)–activated pumps initiated via ligand binding to EC surface receptors, causing activation of G-proteins and increased IP_3 production.[19] Depletion of stored Ca^{2+} stimulates capacitive Ca^{2+} entry (CCE) through the EC membrane. We present a brief history of the development of models related to NO signaling and refer the reader to a recent review of vascular Ca^{2+} dynamics.[34]

Early mathematical models of EC Ca^{2+} dynamics were developed by Wiesner et al.[35,36] and others.[37,38] These models often relied upon parameter values estimated from in vitro experiments using other types of cells. Mechanisms to alter $[Ca^{2+}]_i$ included ligand-receptor binding, Ca^{2+} resequestration, CCE, and Ca^{2+} release pumps.[35] In the second modeling article by Wiesner et al.,[36] 2 mechanisms were used to model effects of WSS stress on $[Ca^{2+}]_i$ by means of agonist mass transfer via perfusion and by increasing EC permeability to extracellular Ca^{2+}.

Silva et al.[39] integrated models for plasmalemma electrophysiology and Ca^{2+} dynamics to predict EC responses to different stimuli and to characterize how V_m varies with $[Ca^{2+}]_i$. The model was able to reproduce EC responses that had been reported in the literature, and it predicted observed effects of external K^+ on hyperpolarization or depolarization of ECs. Effects of WSS on $[Ca^{2+}]_i$ or mechanisms causing Ca^{2+} oscillations were not modeled. A sensitivity analysis of model parameters was conducted and the range of uncertainties for each parameter was described and model limitations were discussed. As part of their review of atherosclerosis and EC Ca^{2+} signaling, Plank et al.[40] developed a model incorporating both mass transport and IP_3-dependent Ca^{2+} dynamics. The model shows that peak $[Ca^{2+}]_i$ depends more on stored Ca^{2+} release whereas the resting plateau $[Ca^{2+}]_i$, and consequently V_m, depend more on Ca^{2+} influx. The model also can generate sustained Ca^{2+} oscillations.

II.B. Modeling Ca^{2+} Kinetics and eNOS Activation

Amongst known NOS isoforms, eNOS is most sensitive to changes in $[Ca^{2+}]_i$,[41] although eNOS activity also can be regulated by Ca^{2+}-independent mechanisms[42–45] Caveolin-1, the major coat protein of caveolae, binds to eNOS,[46] which in turn binds to calmodulin to activate the synthesis of NO. Increased NO leads to increased levels of cGMP, which activates PKG, which is thought to inhibit Ca^{2+} influx, creating a negative feedback loop to control $[Ca^{2+}]_i$.

Production of NO by eNOS was added in a second Ca^{2+} dynamics modeling article by Plank et al.[47] A mathematical relationship between eNOS concentration and WSS was used that previously had been determined in a combined hemodynamic modeling simulation that correlated computed WSS at locations where in vitro confocal measurements of eNOS protein concentration were obtained in rabbit carotid artery samples.[48] The model incorporated effects of increased free Ca^{2+} in the cytosol, which causes eNOS to disassociate from caveolin and become enzymatically active. Based on uniform EC properties, the model characterized concentrations of IP_3, free Ca^{2+}, and buffered Ca^{2+} in the cytosol and Ca^{2+} in internal stores.[47] Comerford et al.[49] further modified this model to predict effects of adenosine triphosphate (ATP) and $[Ca^{2+}]_i$ on eNOS activity in 3-dimensional hemodynamic models of arterial bends and bifurcations with regions of reduced eNOS protein where WSS is low. The resulting spatial variations in eNOS concentration predicted for these geometries are shown in Fig. 2. The strong correlation between WSS and eNOS activity suggests that low Ca^{2+} in these regions is associated with reduced NO bioavailability and has implications for development of atherosclerosis.

Hong et al.[32] developed a 2-dimensional microdomain model that considers the influence of spatial colocalization of eNOS and CCE channels on NO production by ECs. The model suggests that spatial distributions of CCE channels in caveolae microdomains as well as the location of ER relative to eNOS can create significant Ca^{2+} gradients in the EC. The model can explain differential sensitivity of eNOS activation by increased Ca^{2+} from clustered CCE channels or from the ER.

Munaron[50] modeled interaction between NO and arachidonic acid (AA) in Ca^{2+} signaling. The 3-dimensional simulations used Virtual Cell software (available at http://www.nrcam.uchc.edu) with 2 different EC geometries that were determined by imaging BAECS. Calcium diffusion inside the EC caused by plasma membrane Ca^{2+} channels depends not only on the quantitative expression of channels and buffers but also on how they are distributed in specific microdomains. The model suggests that there may be a major effect of channel clusters in thin lamellipodia.[50] It was demonstrated previously by this researcher that low concentrations of AA and NO do not activate release of Ca^{2+} from ER and therefore can be ignored.[51] Changes in NO with AA stimulation also were modeled using information from the literature. However, when eNOS activity was excluded from the simulation, there was no effect on the time course and propagation of the Ca^{2+} response to AA. This model assumed that there are independent ion channels that are activated separately by AA or NO, but the author notes that these specific channels have not yet been identified.

II.C. Shear Stress and Nitric Oxide Production

Shear stress has many effects on ECs, including an increase in $[Ca^{2+}]_i$ and BH_4 with activation of PKs that lead to eNOS activation (see review[19]). Increased NO with higher WSS also has been shown to lead to increased *S*-nitrosylation of at least 12 major proteins in ECs,[52] which may affect multiple signaling pathways. Increased expression of eNOS with high WSS is associated with an increase in the transcription factor nuclear factor κB and a

shear stress response element located in the eNOS gene promoter. The transcription response to increased WSS is under negative feedback control because NO inhibits nuclear factor κB activation.[53] Production of other potential vasodilators, including prostacyclin, c-type natriuretic peptide, and adrenomedullin, also is increased in ECs exposed to shear stress, whereas production of the vasoconstrictor angiotensin II decreases.[19] In studies of mouse carotid artery in which tapered casts were placed to alter WSS in the blood vessel, eNOS was upregulated within 1 day and reached steady state levels in 2 days in regions with augmented WSS.[48] An in vitro study using ovine fetoplacental artery ECs grown to confluence at 3 dyn/cm^2 then subjected to higher pulsatile shear stresses for up to 24 hr has shown that acute increases in NO production are attributed to eNOS activation whereas longer-term increases in pulsatile shear stress are associated with increased eNOS expression and NO production.[54] At the highest WSS (25 dyn/cm^2) investigated, there was an 8-fold increase in NO production that exceeded the increase in eNOS protein (3.6-fold increase) and eNOS messenger RNA (1.5-fold increase).

Information about the effects of WSS on NO production has come primarily from in vitro studies with cultured ECs. A combined imaging and porphyrin/Nafion-coated carbon fiber NO microelectrode study reported transient increases in NO with changes in WSS.[55] The NO sensor was positioned at a distance approximately 100 mm above the surface of a monolayer of cultured BAECs. The measured NO reached a peak within 1 to 3 s after the peak increase in $[Ca^{2+}]_i$ following a step change in shear stress under laminar flow conditions. Peak NO increased as a linear function of the magnitude of the change in WSS in the range of 0.2 to 10 dyn/cm^2. Following each step change in flow, NO returned to roughly the same level.

Fadel et al.[56] used a linear relationship linking shear stress (τ) and NO production in a series of time-dependent simulations for an NO-producing monolayer of ECs in a parallel-plate flow chamber. A nonlinear, power law relationship between shear stress and NO production was also examined:

$$R_{NO} = R_{Basal} + B\left(\frac{\tau_{wall}}{\tau_{ref}}\right)^m$$

where R_{Basal} is the basal rate of NO production at zero shear stress, and B and m are parameters used to represent the influence of shear stress on NO production relative to a reference shear stress (τ_{ref}). The power m was set to either 1/3 (nonlinear model) or 1 (linear model) in both transient and non-time-dependent simulations. Although linear and power law relationships may be useful over limited ranges of shear stress, these functional relationships may not be accurate at higher WSSs outside the range investigated experimentally. The model predicts that NO gradients are very steep in the flow stream near the EC surface, except at very low flow rates. Steady state NO values are affected strongly by convection, so that high NO values are generated at low flow rates and decrease with higher flow rates. The model suggests that interpretation of NO microelectrode measurements in the flow chamber would require precise knowledge about the position of the sensor tip in the flow stream due to the very steep NO gradients. However, the relationship between NO concentration and NO production is constant for any fixed position.

In their model of a commercially available parallel-plate flow chamber for cultured ECs, Plata et al.[57] use a sigmoidal function for R_{NO} as a function of shear stress

$$R_{NO}=\frac{R_{NOmax}}{1+Aexp^{-B\tau}}$$

where R_{NOmax} is the maximum NO production rate and A and B are constants. This is a saturating model that approaches a maximum rate at very high WSSs. The basal rate (at zero shear stress) for this model is $R_{basal} = R_{NOmax}/(1+A)$.

This functional relationship assumes that R_{NO} is related to eNOS expression directly and is based on in vitro confocal microscopy measurements of eNOS-green fluorescent protein expression at different locations in mouse carotid artery where large spatial variations in WSS were created after placing a tapered cast around the blood vessel.[48] The green fluorescent protein signal was correlated with WSS at each measurement site as determined from computational fluid dynamics modeling of blood flow in the tapered vessel. Other studies using pharmacologic agents to alter eNOS expression were also done, showing a similar sigmoidal relationship between eNOS expression and WSS.[58] Experimental data were obtained from blood vessels removed from animals where ECs were continuously exposed to in vivo WSS levels for relatively long time periods (days). A negative feedback term that is linearly proportional to NO also was added to the nonlinear function, which has an effect on eNOS transcription with long-term exposure to higher WSS.[57] Despite differences in the design and physical dimensions between flow chamber models developed by Fadel et al.[56] and Plata et al.[57] predicted NO gradients in the chamber were similar using NO production rates reported in the literature. The model developed by Plata et al.[57] did not include a time delay between the onset of WSS and completion of transcriptional changes. The sigmoidal function for the relationship between R_{NO} and WSS may not be the optimal function to use for cultured ECs that are subjected to acute changes in WSS for relatively short time periods without sufficient time for changes in eNOS expression. Either model can be modified using other assumed relationships of R_{NO} with WSS; however, both chamber models need to be verified by comparing experimental results with model predictions.

We have conducted a flow chamber study with cultured bovine BAECs to measure changes in NO at different shear stresses in the range of 0.1 to 20 dyn/cm^2,[59] using our chamber model[56] to interpret the experimental data. The relationships for R_{NO} with τ described above did not provide the best match to our NO measurements. Instead, a hyperbolic relation

$$R_{NO}=R_{NObasal}+R_{NOmax}\left(\frac{\tau}{\tau+A}\right)$$

with $R_{NObasal}$ = 2.13 nM s^{-1}, R_{NOmax} = 457.5 nM s^{-1} and A = 35 dyn/cm^2 gave a better fit. This model predicts that the value for R_{NO} = 104 nM s^{-1} at τ = 10 dyn/cm^2 for these ECs.

This study emphasizes the importance of modeling NO transport within the experimental system to utilize NO sensor measurements to determine actual NO production rates. However, there is a need for the incorporation of mechanistic models of mechanotransduction events and signaling processes leading to NO production in response to shear stress. Real-time NO measurements will allow comparison of predicted changes in the kinetics of response when elements of the signaling system are experimentally modulated.

II.D. Integrated Models for Blood Vessels

A network model of the coronary circulation consisting of 10 resistance compartments in series was developed by Cornelissen et al.,[60] which included NO-dependent flow dilation, metabolic flow control, and myogenic mechanisms to predict changes in vascular tone in the network. The spatial distribution of NO in the network was not modeled explicitly. Mathematical relationships used in the model were based on experimental data obtained from different sizes of isolated porcine coronary arterioles[61,62] that quantified changes in diameter with luminal pressure, as well as diameter changes with NO generated from nitroprusside. In these studies, arterioles with diameters of approximately 165 μm were found to be the most sensitive to shear stress, and smaller arterioles of approximately 100 μm in diameter had the strongest myogenic responses. It should be recognized that these in vitro experiments were conducted in the absence of blood, so they may have limitations when extrapolated to in vivo conditions. Vascular wall tension was represented by a thin wall (law of Laplace) model. A Hill model relationship was used to vary a flow-dependent parameter as a function of NO, based on the experimental nitroprusside studies, with the NO concentration at 50% of the response estimated to be 93 nM. Another nonlinear function for the relationship between NO and shear stress also was derived from the experimental data. However, this function was saturated for $\tau > 4$ dyn/cm^2. An attenuation factor was introduced into the model to shift the NO-shear stress relationship to higher τ to better represent in vivo conditions. The authors concluded that there was a balance between upstream flow-dependent dilation due to NO and downstream constriction with metabolism. The model predicted that the myogenic mechanism has a significant contribution toward the control of blood flow.

To better understand signal transduction mechanisms, Kapela et al.[63–65] developed a blood vessel model with intracellular signaling between neighboring cells in the vascular wall. A 3-mm-long rat mesenteric arteriole segment was modeled with anatomically appropriate arrangements of ECs and smooth muscle cells (SMCs). Individual cells were connected by gap junctions permeable to Ca^{2+}, K^+, Na^+, and Cl^- ions and IP_3. The model also included effects of NO. The model simulates local changes in V_m when either ECs or SMCs are stimulated electrically or chemically, based on gap junction connectivity between cells. Signaling cascades generate contrasting responses depending upon which side of the vessel is stimulated. When the SMC side is stimulated, a biphasic V_m response is predicted, whereas when the EC side is stimulated, there is a moderate effect on conduction of signals initiated within the endothelium. Inhibition of IP_3 diffusion is predicted to abolish EC Ca^{2+} spreading and reduce the total number of ECs with open channels. The model also predicts that Ca^{2+} diffusion through gap junctions does not increase $[Ca^{2+}]_i$ levels. It should be noted that some gap junction parameters for ion transport between different cell types in the model have not yet been experimentally determined.

II.E. Experimental Studies of Ca^{2+} and Nitric Oxide–Dependent Conducted Vasomotor Responses

Local changes in blood flow to tissue not only require changes in arteriolar tone, but also in larger upstream feed vessels. Conducted vasomotor responses are thought to provide a signal from metabolically active tissue to the upstream blood supply.[66–68] Uhrenholt el al.[69] demonstrated in isolated hamster retractor muscle feed arteries that an acetylcholine (ACH) stimulus caused a decrease in SMC $[Ca^{2+}]_i$ with rapid upstream and downstream propagation of Ca^{2+} waves in ECs for distances >1 mm at a velocity of ~111 mm/s, which is much faster than velocities measured in EC cultures in the literature. Maximum dilation using a NO donor reduced the distance traveled by propagated Ca^{2+} waves to approximately 300 μm. Another study by this group used Ca^{2+} imaging to investigate effects of inhibiting NO production in isolated, perfused rabbit renal arterioles, which have ECs and only a

single layer of SMCs.[70] Only increases in EC $[Ca^{2+}]_i$ were observed following stimulation by ACH. Depolarization by perfusing the arterioles with high K^+ caused vasoconstriction with large increases in SMC $[Ca^{2+}]_i$ and more modest increases in EC $[Ca^{2+}]_i$. In untreated arterioles with normal NO production, there was an initial contraction with high K^+, followed by relaxation despite sustained elevation of SMC $[Ca^{2+}]_i$. Vasoconstriction with high K^+ was significantly greater in arterioles treated with the nonspecific NOS inhibitor N^w-nitro-L-arginine methyl ester (L-NAME). Vessels remained constricted during perfusion, although there was no difference in the increase in SMC $[Ca^{2+}]_i$ compared with untreated arterioles. The authors speculated that NO is affecting Ca^{2+} sensitivity of the SMC contractile apparatus through cGMP-dependent stimulation of myosin light change phosphatase.

In an in vivo study, Figueroa et al.[71] investigated activation of Ca^{2+} channels and long-distance signaling in electrically stimulated mouse cremaster arterioles in wild-type and eNOS-knockout mice. As shown in Fig. 3, changes in arteriolar diameters were quantified at the stimulation site and at more distant locations, and different experimental manipulations were done, including damaging the endothelium at the stimulation site by air embolism and pharmacologic inhibition of NO production. Damaging the endothelium significantly reduced resting diameters and propagated responses (Fig. 3A). Resting diameters also were significantly reduced after inhibiting NO production, with smaller changes in diameter during stimulation both locally and at more distant locations (Fig. 3B). Conducted responses were still present in the eNOS-knockout mice, but were smaller both locally and at more distant locations compared with responses from wild-type mice (Fig. 3C). Another in vivo study measured local and conducted responses to ACH or adenosine in arterioles in the cremaster muscle microcirculation of wild-type and connexin 40-deficient mice.[72] These studies demonstrate that the ACH response is propagated through ECs, whereas the response to adenosine is propagated through SMCs, independent of NO. In connexin 40-deficient mice, ACH-conducted responses were attenuated at longer distances from the local stimulation site, whereas adenosine-conducted responses were no different compared with wild-type mice. Other studies in mouse cremaster muscle examining effects of local changes in tissue oxygenation also report NO-independent conducted vasomotor responses, based on inhibition of NO production, with evidence that ATP-sensitive K^+ (K_{ATP}) channels play an important role.[73,74]Future research efforts need to be directed toward obtaining a better understanding of the physiological and molecular mechanisms that regulate eNOS activity, including how shear stress modifies endothelial function. Though EC culture studies may continue to be useful for exploring these mechanisms, in vivo EC behavior needs to be better characterized using appropriate experimental designs. At the present time, integrated models for vascular networks may be premature and difficult to truly validate by comparing theory with experimental measurements.

III. SOLUBLE GUANYLATE CYCLASE AS PRIMARY TARGET OF NITRIC OXIDE

Soluble guanylate cyclase (sGC) generally is recognized to be the primary target for NO, which rapidly activates the conversion of guanosine triphosphate (GTP) to the second messenger cGMP after binding to the ferrous iron atom in the β-subunit, with resulting relaxation of vascular smooth muscle.[75] Estimates for the NO concentration at half-maximal activation (EC_{50}) of sGC range from 1 to 250 nM.[76–81] It now seems that sGC regulates 2 types of cGMP signals: a tonic response to basal NO levels that is long lasting and produces low levels of cGMP, and an acute response that can generate a shorter, large increase in cGMP synthesis (see review[82]).

III.A. Models for Soluble Guanylate Cyclase Activation

A model for activation of sGC by Yang et al.[83] assumes NO binding at 2 sites with a negative feedback loop based on cGMP concentration to inhibit sGC activity. This modeling approach results in a Michaelis-Menten type of relationship between NO and cGMP that can be shifted toward increased sensitivity at lower NO concentrations. The model predicts how intracellular Ca^{2+} might vary as NO affects sCG activity, based on cGMP activation of large conductance K^+ or Ca^{2+} ion channels, which in turn predicts how the relative force generated by smooth muscle might vary. However, the authors noted that there are many other mechanisms that were not included in the model that also have an impact on activation of sGC by NO.

Also, ATP, nucleotides, and purine-like molecules affect the sGC catalytic site (see review[82]), and ATP has been shown to inhibit sCG activity.[84,85] An enzyme-linked receptor model for sGC activity, analogous to modeling of a G-protein receptor (adenylyl cyclase), has been developed by Roy et al.[77], which characterizes interactions with ATP, GTP, and the allosteric enhancer YC-1. The model was fitted to experimental data obtained with purified bovine lung sGC. In the presence of 100 μM GTP, the EC_{50} for NO was 3.4 nM with 1 mM ATP. With higher ATP concentrations (up to 3 mM), activity was inhibited with a right shift (higher EC_{50}) in the inhibition curve. With ATP < 1 mM, which can occur during hypoxia, sGC activity was increased with a left shift (lower EC_{50}) in the inhibition curve. The low NO concentration required for activation of sCG from this study was cited by Hall and Garthwaite[6] to support their view that the normal physiological concentration for NO should be very low. As reviewed by Garth-waite,[86] the inhibition of sGC by ATP may create a sink for NO, serving to direct NO diffusion toward the signaling target.

III.B. Nitric Oxide Transport Models Based on Soluble Guanylate Cyclase Activation

Mass transport models have been developed to confirm whether NO in the vascular wall is sufficient to activate sGC, guided by available information on the EC_{50} for activation. A comprehensive review of different mathematical models for NO transport was published recently by Tsoukias.[87] As reviewed by Buerk,[88] the rapid uptake of NO by Hb in red blood cells (RBCs) was recognized to be a critical parameter that had a profound effect on NO bioavailability in early NO transport models.[89–94] It appeared that only a small fraction of the NO produced by the endothelium could escape Hb scavenging reactions to reach the vascular wall. Several NO transport models included diffusion barriers around the RBCs and in the RBC-free plasma gap in the bloodstream near the endothelium to limit NO diffusion into the RBCs.[95–102] In general, NO biotransport models have used hematocrit-dependent NO scavenging rates that are approximately 2 orders of magnitude lower than the rate for free Hb. NO scavenging by Hb is still so rapid that convective transport of NO is negligible compared with diffusion. One exception was a planar diffusion and convection model for a renal arteriole that predicted significant amounts of NO can be transported downstream because the assumed half-life for NO was relatively long compared with the blood flow transit time used in this model.[103]

Another major parameter in NO transport models is the rate of NO production (R_{NO}) by eNOS, usually assumed to be a constant or variable depending on the wall shear rate. NO also can be produced by other NOS enzymes. Units for R_{NO} are $\mu M\ s^{-1}$ on a cell volume basis, or in some modeling articles is represented by an exchange rate (NO flux or NO release) from the endothelium with units of $\mu M\ cm^{-2}\ s^{-1}$. R_{NO} values for eNOS are in the 10 to 12 $mM\ s^{-1}$ range, depending on shear stress, based on measurements of metabolic products nitrite (NO_2^-) and nitrate (NO_3^-) generated by cultured ECs.[45,104] However, a model for predicting R_{NO} based on kinetic rates for in vitro cultured EC studies and other biochemical measurements from the literature predicted much lower values for R_{NO} ranging

between 0.01 and 0.095 mM s^{-1}.[105] This may reflect differences in eNOS expression and function in vitro, which may be much lower than in vivo or in situ. Based on an analysis[106] of in vitro experimental NO microelectrode measurements from aortic vessel segments,[107] values for R_{NO} of 70 mM s^{-1} or higher have been used in mathematical models for NO transport. However, it is still not clear how much NO must be produced by the endothelium to control vascular tone. There is experimental evidence from in vitro studies with mouse aorta that the efficacy of NO in producing vasodilation depends on how Ca^{2+} is mobilized in vascular smooth muscle.[108] A second, non-cGMP-dependent pathway may be involved.

In contrast to the majority of models that use constant, steady-state R_{NO}, Tsoukias et al.[109] simulated the effects of periodic, transient bursts of NO, modeled as a 10-s duration square wave with 25-nM amplitude and 30-s period (frequency = 2 per min, or ~0.03 Hz). The model predicted an enhancement of sGC activity compared with sustained NO production. Furthermore, the model predicted that it is possible to activate sCG with a smaller NO release rate and reduce the effects of NO scavenging by Hb in the bloodstream or NO scavengers in tissue (e.g., myoglobin). They speculated that NO oscillations may be associated with Ca^{2+} oscillations in the endothelium.

Kavdia and Popel[110] modeled how large reductions in hematocrit following transfusion of volume expanders can influence NO bioavailability in the vascular wall of a 50-μm-diameter arteriole. A linear relationship between NO production by eNOS and WSS was used. For the parameters used in their model, WSS = 24 dyn/cm^2 generated a peak NO value of approximately 101 nM in the endothelium, with slightly lower values in the vascular wall of the arteriole as NO diffused out into tissue. The model predicted that a 50% reduction in hematocrit increased endothelial NO to 167 nM, which can be attributed to the combination of reduced scavenging of NO by Hb in the bloodstream along with an overall increase in WSS as blood viscosity is reduced and blood flow increases. However, it is possible to have an overall decrease in WSS with reduced blood viscosity if the increase in blood flow is not large enough. They also modeled effects of transfusion of Hb-based O_2 carriers (HBOCs) on NO. In contrast, much lower NO values were predicted despite an increase in blood flow with reduced blood viscosity. This is consistent with a model by Tsoukias and Popel,[111] who predicted that NO scavenging by blood containing 5 g/dL free Hb is approximately 2 orders of magnitude greater than NO scavenging by RBCs at a normal hematocrit of 45%. HBOCs are small, (typically ~0.1 μm diameter) and can enter the normally RBC-free plasma layer near the endothelium. Also, there is no diffusion barrier as attributed to the diffusion-limiting blood plasma boundary layer around larger RBCs.[92,111,112] The model prediction is consistent with a higher scavenging of NO in the blood by HBOCs, which has clinical relevance for possible systemic hypertension and vasoconstriction with HBOC transfusion. However, it is not clear whether increased NO scavenging contributes to the adverse events reported in clinical trials of HBOCs.[113]

Some models include a region of capillaries near the arterioles or between arteriole-venule pairs, which can act as a sink for NO because of scavenging by Hb in the RBCs,[109] or it can act as either a sink or source that influences NO diffusion near arterioles and venules,[98,114] depending on NO production from capillary endothelium or from other sources in tissue. Models have also been developed showing the interaction between NO and O_2^-, which can reduce NO bioavailability significantly and generate $ONOO^-$ in the vascular wall and surrounding tissue.[101,115,116]

Preliminary work has been done to develop NO transport models for microcirculatory networks.[117] A model to predict effects of changes in WSS and flow-related hematocrit distributions on NO was developed for a 3-dimensional geometry using published microcirculatory data for hamster cheek pouch. NO concentration profiles in a 100 μm ×

500 μm × 75 μm volume of tissue containing 2 arteriole-branching trees and 9 capillaries supplied by the arterioles were computed using finite element methods, as shown in Fig. 4A. Distributions for WSS and RBCs in this branching network were heterogeneous, depending on flow conditions. Details for the spatial variation in WSS in the 2 arterial branching trees are shown in Fig. 4B, where regions of low WSS are present. In some simulations, the model predicted that an arteriolar branch with high flow and high R_{NO} could have lower NO in the vascular wall than the other branch (Fig. 4C). Diminished NO in the vascular wall also could be simulated with a higher scavenging rate of NO due to a higher hematocrit resulting from RBC redistribution at the vessel bifurcation. The model also predicted that low WSS and low eNOS activation at other locations could have higher vascular wall NO caused by reduced NO scavenging rates with lower hematocrit resulting from blood phase separation.

III.C. Experimental Measurements of Vascular Wall Nitric Oxide Bioavailability

Optical measurements of NO using diaminofluorescenin (DAF) or other NO-sensitive dyes are useful for identifying anatomical locations where NO is being produced or where R_{NO} is changing in response to a stimulus. For example, Kashiwagi et al.[118] reported that, in addition to production from eNOS, NO also was produced by nNOS in nerves around arterioles (but not venules) in the rat mesentery, based on their optical measurements. Another DAF study of the mesenteric microcirculation found 50% lower NO levels in the microvascular walls of streptozotocin (STZ) diabetic rats compared with normal rats.[119] Results for arteriolar-venule pairs in this study suggested that NO from the venule was influencing arteriole tone. Interestingly, no correlation was found between WSS and NO in arterioles in either normal or STZ-diabetic rats. However, a correlation between WSS and NO in venules was found for normal rats, but not in STZ-diabetic rats. Also, activated leukocytes adhering to venular walls caused a reduction in NO in normal rats, presumably because of the release of O_2^- and scavenging of NO, but had little effect in STZ-diabetic rats, suggesting that O_2^- levels were elevated. A DAF study of hemorrhagic shock (blood pressure reduced to 40 mm Hg for 20 min) in rat mesentery reports that venular endothelial NO production is reduced significantly within 30 min after restoring blood volume, with no difference from controls after 24 hr of recovery.[120] An increase in NO production in mast cells was observed after 24 hr, which could be attributed to NO production from iNOS. However, it is not possible to determine absolute NO levels in the microcirculation from any of these in vivo DAF studies. There are many technical issues, such as nonuniform distribution of DAF in tissues or cells and interference from other chemical species, that must be solved before reliable, quantitative optical measurements of NO can be made in vivo.[121–127]Chemiluminescence analysis of superfusate over a hamster cheek pouch preparation has been used to quantify in vivo NO production from a microcirculatory bed, demonstrating an increase in NO production following topical application of platelet activating factor (PAF).[128] The same group used the chemiluminescence method to demonstrate that there is an 83% reduction in NO production after inhibiting NOS that was associated with a 28% reduction in blood flow in the cheek pouch microcirculation.[129] They also demonstrated increased NO production from the cheek pouch following topical application of ACH, which was reduced after treatment with a NOS inhibitor.[130] Although the chemiluminescence technique generated quantitative information about global NO release from the microcirculation, it was not possible to discriminate between rates of NO production from tissue or microvessels.

Electrochemical methods have been employed in a number of microcirculatory studies for more localized measurements with rapid temporal resolution. In vivo experimental NO microsensor measurements of perivascular NO values are generally much higher than predicted by most mathematical models for NO transport in the literature. For example,

Bohlen[131] measured in vivo perivascular NO levels in a superfused rat mesentery and small intestine preparation, reporting mean (±SEM) values of 353 ± 28 nM around arterioles and slightly higher values (401 ± 48 nM) around venules. Vukosavljevic et al.[132] measured similar NO levels in the same microcirculatory preparation, averaging 338 ± 40 nM around arterioles, with slightly lower values of 313 ± 48 nM around venules. In another rat study, even higher NO values, averaging 522 ± 33 nM near arterioles with diameters averaging 53.2 ± 1.6 mm, were reported.[133] An example of NO mapping in a microcirculatory network (superfused rat mesentery and small intestine) conducted in our laboratory (unpublished) using this technique with Nafion-coated recessed NO microelectrodes is shown in Fig. 5, with NO values indicated at each measurement site (circles). In these studies, the zero current (background current) was obtained in the bath far from tissue, assuming negligible NO in the bath. The polarographic current increased as the NO microelectrode was advanced toward the vessel. Examples of experimental measurements near a venule, an arteriole, and a capillary-perfused location are shown at the bottom of Fig. 5.

An earlier study with larger blood vessels in dogs, in which an NO sensor was introduced into the bloodstream via a catheter with the tip positioned near the endothelium, reported baseline values of approximately 154 nM in femoral artery.[134] and approximately 90 nM in femoral vein.[135] NO measured near the dog femoral artery endothelium increased more than 2-fold to approximately 358 nM with infusion of ACH and approximately 420 nM with bradykinin (BK). L-NAME reduced the baseline NO by only 20% but significantly reduced responses to ACH and BK, although both responses were still large (increases >100 nM). It is not clear if the electrodes in these studies might have been sensitive to flow artifacts.

An NO microelectrode study in the hamster cheek pouch microcirculation found much different responses between arterioles and venules with pharmacologic stimulation.[136] Topical application of ACH caused large increases in perivascular NO near arterioles, but no increase was observed for venules. On the other hand, PAF caused large increases in perivascular NO near venules, but not near arterioles. In vitro studies with cultured bovine postcapillary ECs confirmed that PAF stimulated NO production whereas ACH did not. Thus, the increase in NO with PAF or ACH measured previously using chemiluminescence analysis of the superfusate[128,130] did not reflect increases in NO from the entire cheek pouch microcirculation, but were the result of differential responses from arteriolar and venular segments.

One in vivo NO microelectrode study reported that there is a substantial amount of NO (200–600 nM) in the luminal blood of 50- to 70-μm-diameter arterioles, measured by penetrating through the blood vessel wall.[137] This observation raises the possibility that NO can be transported downstream in the bloodstream and diffuse back into tissue. However, a flow-sensitive NO microelectrode might lead to a measurement error (“stirring artifact”) and the actual NO value in blood might be lower. Most models for NO transport predict low NO values in blood, although higher values have been computed in a diffusion and convection model for an arteriole[138] that compares predicted NO gradients using a lower scavenging rate for NO in blood reported by Azarov et al.[139]

1. Effect of Increased L-Arginine—A study by Wagner et al.[140] speculated that rat mesenteric venules should have a higher capacity for NO synthesis in vivo than arterioles because cultured ECs derived from venules were found to have greater NOS activity, with higher intracellular *L*-arginine and eNOS enzyme levels compared with cultured ECs from arterioles. This suggested that there could be differences in both *L*-arginine availability and regional NO production along the microvascular network. Because blood plasma and intracellular *L*-arginine concentrations (millimolar range) are much higher than the K_m for eNOS (micromolar range), the substrate for NO production by ECs should be at saturating

levels. However, exogenous *L*-arginine has been shown to increase NO production (reviewed by Forstermann et al.[141] and Bode-Boger et al.[142]), a phenomena known as the "*L*-arginine paradox." For example, in vivo microelectrode measurements of perivascular NO demonstrated that topical application of 100 mM *L*-arginine caused a significant increase in NO with an increase in tissue perfusion for several minutes.[132] Venules had a slightly larger increase in NO with *L*-arginine compared with arterioles. An earlier study measured similar changes in NO after continuous topical administration of 1 mM *L*-arginine, with a 2-fold increase (baseline, 334 ± 19 to 686 ± 53nM) within 2 to 3 minutes.[131] Similar but faster NO responses were measured using local micropipette superperfusion techniques.[143] The amino acid *L*-lysine, which competes with *L*-arginine transport via cationic amino acid transporters, caused decreased NO production and blood flow in rat intestinal arterioles,[144] suggesting that *L*-arginine availability is transport-dependent in the microcirculation.

One hypothesis for the *L*-arginine paradox is that the presence of ADMA inhibits NOS activity.[15] Evidence for this hypothesis has been reviewed.[142] Because eNOS is biologically active when colocalized with caveolae on the plasma membrane.[46] another possibility is that compartmentalization of *L*-arginine within cells limits its availability to NOS. There is also evidence that the activation of eNOS by *L*-arginine is a membrane-bound, receptor-mediated process, affecting NO release through a signal transduction mechanism.[145]

2. Effect of Hypoxia—The K_m for O_2 required for NO production by eNOS is relatively low,[146] but NO production could be limited under severely hypoxic conditions. For example, in vitro studies with human umbilical vein ECs exposed to chronic hypoxia (1% O_2) for 24 hr had decreased eNOS expression and lower basal NO release compared with human umbilical vein ECs cultured for 24 hr in 5% or 21% O_2.[147] Interestingly, NO responses to histamine were enhanced after 1 hr of hypoxic exposure but were blunted after chronic hypoxia. However, there are other mechanisms in vivo that can cause hypoxic vasodilation and increase microcirculatory blood flow independent of NO, although higher WSS could then cause an increase in NO production.

An early in vitro study with isolated rabbit femoral artery and aorta segments subjected to luminal hypoxia provided evidence that endothelium-derived relaxing factor is released, with vascular relaxation blocked in the presence of Hb or after removing the endothelium.[148] More recently, in vivo diameter measurements of primary arterioles (diameter ~45 μm) and terminal arterioles (diameter ~10 μm) in rat spinotrapezius muscle have shown that both sizes of arterioles dilate during systemic hypoxia (12% or 8% O_2), with relatively larger responses for terminal arterioles.[149] There was no significant change in arteriolar diameter from baseline after treatment with L-NAME. However, hypoxic vasodilation was attenuated significantly for both sizes of arterioles. Infusing an NO donor restored hypoxic vasodilation for primarily arterioles, but not for terminal arterioles, in animals treated with L-NAME, suggesting that other vasoactive substances (e.g., adenosine) may be involved in hypoxic vasodilation of terminal arterioles. Another in vivo microcirculatory study in electrically stimulated rat spinotrapezius muscle preparation found that L-NAME reduced microvascular diameters as well as responses to electrical stimulation, which could be restored with an NO donor.[150] However, studies with a cyclo-oxygenase inhibitor (indomethacin) reduced the inhibitory effects of L-NAME. Greater effects that were observed for paired arterioles and venules suggest that vasodilatory prostanoids are released from the venules. Increased perivascular NO near rat intestinal arterioles has been measured during acute systemic hypoxia.[133]*L*-lysine was found to suppress increases in NO and blood flow with hypoxia.[144] In a study using normal and obese rats, baseline perivascular NO levels in the obese animals were lower, with

approximately 50% smaller increases in NO during acute hypoxia compared with normal animals.[151]

A number of studies have shown increased cerebrovascular blood flow during hypoxia that implicates NO. A magnetic resonance imaging study with conscious, healthy, human volunteers in which inspired O_2 was reduced to cause hypoxic vasodilation found that infusing a nonspecific NOS inhibitor reduced the increase in cerebral blood flow during hypoxia.[152] A study in rat brain demonstrated that increased RBC velocity observed during hypoxia could be blocked with a specific inhibitor of nNOS.[153] In vivo perivascular NO microelectrode measurements near cerebral arterioles in rat brain during superfusion with low O_2 in the bath reports increased NO during hypoxic vasodilation, and both the increase in vessel diameter and increase in NO can be suppressed significantly using a selective inhibitor of nNOS.[154] Studies of Na^+ and Ca^{2+} ion transporters in the rat cerebral microcirculation using pharmacologic agents found that NO production (primarily by nNOS) and vasodilation could be reduced significantly by suppressing $Na^+/K^+/2\ Cl^-$ exchange or Na^+/Ca^{2+} exchange; altering Na+/H+ exchange had little effect.[155] Similar findings were reported for the influence of ion transporters on NO production by eNOS and hypoxic vasodilation of arterioles in the intestinal microcirculation.[156]

3. Effect of Hyperoxia—Little increase in NO production from eNOS is expected at higher blood pO_2 levels, although increased O_2 availability may have more of an effect on nNOS, which has a higher K_m for O_2 compared with eNOS.[146] In vitro studies with porcine coronary artery segments with NO electrodes positioned in the lumen of the vessels report that hyperoxia reduces luminal NO.[157] Inhibition of NO with ADMA markedly reduced hyperoxic vasoconstriction, and vessels did not constrict with O_2 after removing the endothelium. Vessels that were preconstricted with K^+ also had blunted responses to O_2, suggesting that endothelium-derived hyper-polarizing factors (EDHFs) may also be involved. On the other hand, in vivo NO electrode studies in rats conducted during exposure to hyperbaric O_2 report large increases in NO at perivascular locations near the abdominal aorta, which can be reduced substantially using an inhibitor specific for nNOS, and reduced even more with L-NAME, a nonspecific NOS inhibitor.[158] Additional NO microelectrode studies near the abdominal aorta were conducted under hyperbaric conditions with wild-type, eNOS-knockout, and nNOS-knockout mice, with large increases in perivascular NO found with wild-type and eNOS-knockout mice, but much smaller increases with nNOS-knockout mice. Increased perivascular NO production at 2.8 atmospheres pure O_2 seemed to be an oxidative stress response involving enhanced association of nNOS with calmodulin facilitated by heat shock protein 90[158] and probably not a direct effect of increased O_2 availability.

4. Effect of Hemodilution—Tsai et al.[159] made NO measurements at perivascular locations near arterioles and venules, and in regions of tissue perfused by capillaries in the skinfold of conscious hamsters. NO microelectrode measurements were made before and after animals were exchange transfused with either high- or low-viscosity Dextran solutions, reducing hematocrit from 45% to 11% in both cases. They reported mean (±SEM) perivascular NO values of 632 ± 36 nM for arterioles (mean diameter , 54.9 ± 17.7 mm) prior to transfusion. Figure 6 shows NO measurements and statistical comparisons among vessels and experimental groups, with the most significant differences found when comparing high- and low-viscosity groups. Higher WSS would be expected with the high-viscosity solution. There were significant differences in microvascular hemodynamics depending on final blood viscosities after transfusion, without significant changes in arteriolar or venular diameters. Measured RBC velocity and calculated flow rates were significantly lower in both arterioles and venules for the low-viscosity transfusion compared with the controls before hemodilution. The opposite result was found for high-viscosity

transfusion, with significant increases in measured RBC velocity and calculated flow, especially for venules. Transfusion with high-viscosity solution significantly increased NO levels (>1,000 nM) for both arterioles and venules compared with control blood vessels. In contrast, there was a reduction in perivascular NO measured after transfusion with a low-viscosity solution, although it was not statistically different from control. The first observation is consistent with a reduction in NO scavenging by Hb, although the second observation is not consistent with this explanation. Although the calculated WSS was higher for the high-viscosity transfusion compared with the lowviscosity transfusion, no statistically significant relationship was found between WSS and perivascular NO levels.

III.D. Tissue Nitric Oxide Bioavailability Measurements

NO bioavailability in other tissues is also important for understanding how blood flow and O_2 metabolism are regulated in different organs and for validating NO transport model predictions. Mitchell and Tyml[160] reported indirect experimental evidence that NO is released from capillaries and influences arteriolar tone. Using intravital microscopy, they measured RBC flux and velocity in capillaries in response to BK to stimulate NO production and local application of L-NAME to inhibit NO production. They found that locally applied L-NAME significantly reduced RBC flux and velocity in the capillary but had no effect on the feeding arteriole and draining venule. Locally applied BK, on the other hand, caused pronounced increases in RBC velocity in the capillary and gave rise to remote arteriolar dilation. They concluded that NO is released from capillaries, affecting arteriolar tone.[160] The hemodilution study in hamster skinfold by Tsai et al.[159] found baseline tissue NO levels of approximately 300 nM prior to transfusion in regions perfused by capillaries. Tissue NO was significantly higher in animals transfused with high-viscosity solution and slightly lower in animals transfused with low-viscosity solution. Lower tissue NO levels of approximately 150 nM in regions perfused by capillaries were reported in the rat intestinal preparation.[133] Relatively large, needle-type, commercial NO electrodes have been used to measure tissue NO. For example, a 200-μm diameter electrode with a 3-mm working length (NO-sensitive part) reports average values for NO in rat renal cortex of approximately 231 nM and higher values of approximately 703 nM in the renal medulla.[161] Currents for the zero NO levels were determined using L-NAME. Earlier studies with larger NO electrodes report similar values for rat renal cortex[162,163] and renal medulla.[164]

In vivo NO recordings have been made in the CA1 subregion of the hippocampus in rat brain using Nafion and *o*-phenylenediamine surface-modified, 30-μm-diameter, carbon fiber NO microelectrodes with approximately 200 μm exposed length.[165,166]. Extensive electrode testing was done to ensure that interference from other chemical species (ascorbate, dopamine, NO_2^-, noradrenaline, serotonin) was minimized. In one study, pressure injections of saline solution containing dissolved NO or solution with 100 μM N-methyl-D-aspartic acid (NMDA) were made and changes in tissue NO from baseline were measured.[165] When NO solution was injected approximately 300 μm from the sensor, transient increases in tissue NO were measured with a rise time of 1.5 s and first-order decay rate constant of 0.78 s^{-1}. No changes in tissue NO were observed following local injection of saline without dissolved NO. Local injection of NMDA caused a biphasic NO response in 28% of trials, with a large transient peak followed by a smaller and lower secondary peak. The NO response was frequently smaller for repeated NDMA injections, although it was variable for other repeated trials. Measurements also were made in the striatum, with large transient increases in tissue NO after injecting100 μM NMDA. In a second in vivo study, local injections of 5, 20, or 100 mM glutamate or 0.1, 1, or 5 mM NMDA were made in the CA1 subregion of the rat hippocampus, with peak NO responses reaching 1 μM or higher, depending on the dose.[166] NO responses could be attenuated significantly using inhibitors of nNOS or with antagonists of α-amino-3-hyroxy-5-methyl-4-isoazolepropionic receptors and

NMDA receptors. Baseline NO levels were not reported in either study. The same type of NO sensor also has been used for tissue NO measurements in slices of rat hippocampus.[167,168] In vivo NO recordings also have been made at different depths in the granule cell layer of mouse olfactory cortex using recessed tip, Nafion-coated NO microelectrodes in response to computer-controlled delivery of different odors for 5 s.[169] Peak tissue NO responses increasing to an average of 56.4 nM above baseline were reached by 3.4 s (range, 1.45–5.75 s) after exposure to the different odors. Baseline tissue NO was not determined, only the changes with odor stimulation. In vitro NO microelectrode measurements also were made in mitral and granule cell layers of slices from mouse olfactory cortex in response to different experimental conditions.

In vivo tissue NO responses with simultaneous laser Doppler flowmetry (LDF) have been measured in rat somatosensory cortex using recessed, Nafion-coated NO microelectrodes during electrical stimulation of the contralateral forepaw for 4 s.[170] Peak NO responses were approximately 125 nM above baseline within 400 ms after onset of stimulation, whereas the peak LDF increase occurred at 3.7 s, toward the end of the stimulation period. Tissue NO decreased from the peak during continued stimulation and decreased below baseline as blood flow remained elevated for several seconds after ending stimulation, suggesting that convective washout of NO may be involved. Baseline NO in the somatosensory cortex was not determined.

Very high tissue NO levels (>2 μM) have been measured with recessed, Nafion-coated NO microelectrodes in tumors implanted in immunodeficient mice.[171] which were related to NO production by eNOS and were higher with increasing density of blood vessels. Average NO levels were higher in melanoma tumors grown in cranial windows compared with dorsal skin windows and, in each case, average NO levels were higher in melanoma tumors with higher metastatic potential.Spontaneous in vivo oscillations in tissue NO have been observed in the cat optic nerve head.[172] The amplitudes were approximately 20 nM, with a Fourier analysis showing greatest power at frequencies below 11 per minute (<0.2 Hz), with similar frequencies for tissue perfusion oscillations measured by LDF in the optic nerve head. Inhibition of NO production by L-NAME greatly attenuated the amplitude of the NO oscillations but not the LDF oscillations. It is possible that these observations were caused by transient changes in NO production as described in the mathematical model by Tsoukias et al.[109] or, alternately, caused by vasomotion and periodic changes in shear stress with spontaneous variations in blood flow.

1. Effect of Increased L-Arginine—An in vivo NO microelectrode study found increased renal tissue NO after intravenous injections of *L*-arginine in normal rats, but smaller NO responses were measured in STZ-diabetic rats.[173] The NO response to *L*-arginine in STZ-diabetic rats was reduced by 38% compared with control rats. An in vitro study of NO responses to stimulation by Ca^{2+} ionophore were measured in renal slices and aortic ring segments from normotensive Wistar-Kyoto (WKY) rats, spontaneously hypertensive rats (SHRs), and diabetic rats (SHR treated with STZ) using NO electrodes and electrodes reported to be sensitive to $ONOO^-$.[174] The magnitude of NO responses for both aortic rings and tissue slices were highest in WKY and lowest in the diabetic rats, whereas the opposite finding was reported for $ONOO^-$ measurements, with the highest responses measured with rings and slices from diabetic rats. The NO:$ONOO^-$ ratio was approximately 2 for WKY rats but much lower for SH and diabetic rats, consistent with increased generation of O_2^-. Restoration of endothelial function was found from measurements in tissue samples from STZ-diabetic rats pretreated with nebivolol.

2. Effect of Hypoxia and Ischemia/Reperfusion—Early in vivo studies using an NO microelectrode reported baseline tissue NO of approximately 10 nM in rat brain, with a large

increase in NO > 2 μM with ischemia during middle cerebral artery occlusion.[175,176] An increase in tissue NO above baseline was noted during reperfusion. Differences between normal and SHR rats also were reported, with a smaller increase in NO during occlusion measured in SHR rats with a larger region of infarction.[177] Much different NO responses have been reported for in vivo experiments using larger commercial NO electrodes (diameter ~200 μm) to measure the time course of tissue NO in rat hippocampus during ischemia and reperfusion.[178,179] A large decrease in NO was measured during ischemia, which is consistent with O_2 requirements for NO production by NOS. Baseline NO measurements were approximately 400 nM in this study, with increases in NO of between 700 and 800 nM above baseline during reperfusion. The baseline NO was not characterized in the other study, but the average peak NO increase during reperfusion was 768 nM above baseline.[179]

3. Effect of Hyperoxia—Studies in rat brain using H_2 clearance methods to measure blood flow and microdialysis probes to measure NO metabolites (NO_2^- and NO_3^-) in brain tissue (substantia nigra and caudate putamen) provided evidence that brain tissue NO is increased during hyperbaric O_2, especially at higher pressures.[180] At 4 atmospheres pure O_2, there was a decrease in blood flow and a decrease in NO metabolites in both regions of the brain, but the opposite was observed at 6 atmospheres, with a 200% increase in blood flow and a 150% increase in NO metabolites. These changes were blocked in animals treated with L-NAME. An in vivo NO microelectrode study in the cerebral cortex of rats and mice exposed to 2.8 atmospheres for 45 min confirmed that brain tissue NO increases with hyperbaric O_2.[181] Additional NO microelectrode studies in wild-type, eNOS-knockout, and nNOS-knockout mice, and in wild-type mice treated with a nNOS-specific inhibitor, showed that nNOS is the primary source of NO. The increase in brain tissue NO could be attenuated by superoxide dismutase, by an NMDA receptor antagonist, or by a Ca^{2+} channel blocker delivered during hyperbaric O_2. Immunoprecipitation studies found an increased association between nNOS and heat shock protein 90 during hyperbaric O_2 at these pressures.[181] More recently, a hyperbaric O_2 study in rat brain using H_2 clearance methods to measure blood flow in animals treated with either sildenafil or tadalafil (phosphodiesterase inhibitors) to prolong NO bioavailability reported that greater increases in blood flow were found compared with untreated animals exposed to 4 or 6 atmospheres pure O_2.[182] An initial decrease in blood flow was observed at 4 atmospheres, with a secondary rise above baseline after 30 min of hyperbaric O_2 for treated animals but only a decrease in blood flow for untreated animals. At 6 atmospheres, the increase in blood flow was greater than for untreated animals. The increase in blood flow and O_2 delivery to the brain associated with increased NO seemed to cause more rapid development of central nervous system O_2 toxicity because the time for onset of convulsions was faster in treated animals compared with untreated animals.

Future studies need to address whether the relatively high NO values obtained in many experimental studies are accurate. Though some investigators have paid attention to minimizing interference from other chemical species using various membrane modifications on their NO sensors, the possibility that these electrochemical measurements have been influenced by other oxidized species cannot be ruled out. However, relative changes in NO may still provide insight into physiologic mechanisms, especially if these measurements are repeated after inhibiting NO production or investigated in different NOS-knockout animal models. Advances in development of NO-sensitive dyes also may be forthcoming, and experiments using both electrochemical sensors and optical methods may lead to better quantification of NO under different physiological conditions. Parameters used in NO transport modeling may need to be adjusted, if the accuracy of NO measurements can be established, so that the apparent discrepancy between theory and experiment in the current literature can be resolved.

IV. CYTOCHROME OXIDASE AS A SECONDARY TARGET OF NITRIC OXIDE

It has been known for some time that NO competes with O_2 and reversibly inhibits mitochondrial O_2 consumption by the terminal respiratory chain enzyme cytochrome *c* oxidase.[183–186] As reviewed by Taylor and Moncada,[184] NO is consumed when tissue pO_2 is high; thus cytochrome *c* oxidase is a sink for NO. However, when tissue pO_2 is low, the inhibitory effect of NO on respiration is a protective mechanism against hypoxia, acting to conserve limited O_2 availability.

IV.A. Models for Inhibition of O_2 Consumption by Nitric Oxide

This dependence has been modeled as a simple competitive inhibition, given by a Michaelis-Menten model:

$$VO_2 = VO_2\,\max \frac{O_2}{O_2 + apparent \quad K_m}$$

where VO_2max is the maximum O_2 consumption rate with a linear relationship for the increase in apparent K_m for O_2 consumption with NO:

$$apparent \quad K_m = K_m\left(1 + \frac{NO}{k_{NO}}\right)$$

where K_m is the Michaelis constant in the absence of NO. The above relationship for the apparent K_m and a value for k_{NO} of 27 nM was proposed in a review by Buerk[88] based on limited experimental results in the literature.[185,187] From this analysis, the apparent K_m doubles when NO = 27 nM. Hall and Garthwaite[6] discuss an identical model that has a much stronger dependence on NO, with the apparent K_m doubling at NO = 0.225 nM. A comparison of the 2 models is shown in Fig. 7.

A single catalytic site model for inhibition of O_2 consumption developed by Antunes et al.[188] also is based on purely competitive molecular mechanisms at the heme O_2 binding site. This model predicts that inhibition of mitochondrial O_2 consumption is greater for a high O_2:NO ratio, with a much lesser effect when tissue pO_2 is low. The single-site model also predicts that NO is a weaker inhibitor when O_2 consumption and enzyme turnover is low. Mason et al.[189] propose a 2-site mechanism, where an adjacent copper site can bind NO at lower affinity with noncompetitive kinetics. They reported that NO inhibition of cytochrome *c* oxidase activity was strongly dependent on enzyme turnover, which is consistent with the single-site competitive model by Antunes et al.[188] However, only the 2-site model was able to describe the full range of data obtained in their study.[189] At low turnover rates, they found that cytochrome *c* oxidase activity was half-maximal when NO = 84 nM, but at high turnover rates, half-maximal activity occurred when NO = 1170 nM. The 2-site model predicts that NO is a more effective inhibitor than the single-site model, especially when O_2 consumption is low.

IV.B. Models for Coupled O_2 and Nitric Oxide Transport

There have been relatively few attempts to incorporate NO inhibition of O_2 consumption into mathematical models for O_2 transport. The first model to include inhibition of O_2 consumption by NO was described for vessels in planar geometry by Thomas et al.[190] using experimental estimates for NO scavenging rates in tissue. Our models for coupled NO and O_2 transport in cylindrical geometry for small arterioles for a wide range of conditions

include reversible inhibition of O_2 metabolism by NO.[95,96,98,101,102,191] In general, these models demonstrate that when the source of NO is primarily from the endothelium, O_2 consumption is inhibited to a greater extent in the region of tissue nearest the endothelium, where NO levels are higher, compared with distances farther away because NO disappears as it is scavenged in the surrounding tissue. However, even a small degree of inhibition of O_2 consumption in the well-oxygenated region closest to the arteriole allows more O_2 to diffuse deeper into the surrounding tissue, preventing more hypoxic conditions at deeper locations. This effect is predicted to be even greater in models that include additional NO production by mitochondrial NOS or iNOS in surrounding tissue.[101,102]

IV.C. Experiment Evidence for Inhibition of O_2 Consumption by Nitric Oxide

Earlier studies report increased O_2 consumption in heart,[192] kidney,[193,194] and hind limb preparations[195] after inhibiting NO production, although one study reported a 23% to 34% decrease in myocardial O_2 consumption in canine heart[196] and another reported no change in porcine heart[197] after inhibiting NO production. More recently, a study in conscious, pregnant canines found that inhibition of NO production caused a 49% increase in myocardial O_2 consumption compared with studies in pregnant canines that were conducted without inhibiting NO production.[198] Pregnancy caused an increase in eNOS in the left ventricle, a 55% increase in cardiac output, and increased transcardial NO metabolites, with a shift in metabolism toward greater free fatty acid oxidation and a decrease in glucose oxidation compared with female canines that were not pregnant. The metabolic changes with pregnancy were reversed after treatment with L-NAME, with an increase in glucose oxidation and a decrease in free fatty oxidation. It seems that the increase in NO in the canine heart during pregnancy enhanced the ability of NO to regulate blood flow and control myocardial substrate utilization in these studies.

A dual NO and O_2 electrode study in slices of rat hippocampus recently found that local NMDA stimulated NO production and inhibited O_2 consumption.[167] Tips of individual NO and O_2 electrodes were positioned into the slice with a separation of approximately 50 μm. Figure 8A shows individual NO responses to 10, 50, or 100 μM NMDA, which provoked an increase in NO to as high as 356 nM above baseline (with 100 μM NMDA) and caused a delayed increase in tissue O_2. The maximum NO and increase in O_2 followed a similar trend (Fig. 8B) that was consistent with NO-dependent inhibition of tissue O_2 consumption. A specific inhibitor of nNOS reduced the peak increase in NO with NMDA by 58.5%, with a similar reduction for the increase in O_2 by 50.9%. This study also found that inhibition of O_2 consumption by NO seemed to be reversible with small increases in NO, but was irreversible for the highest peak NO changes with 100 μM NMDA.

In vitro studies with isolated aortic, pulmonary, and mesentery blood vessels from rats and mice determined how the apparent K_m for vascular wall O_2 consumption was affected by NO.[199] The apparent K_m was in the range of 20 to 30 mm Hg pO_2 for control conditions, and decreased into the 7 to 13 mm Hg range after inhibiting NO production or removing the endothelium. After stimulating NO production with either ACH or BK in the bath, the apparent K_m increased into the 40 to 80 mm Hg range and even higher in the 70 to 113 mm Hg range using an NO donor.

Inhibition of O_2 consumption in the vascular wall and surrounding tissue by NO may provide an explanation for differences in intra- and extravascular pO_2 measured by noninvasive O_2 phosphorescence quenching measurements through dorsal chamber windows in conscious wild-type and eNOS-knockout mice.[200] The pO_2 was found to be significantly lower in arterioles, tissue, and venules in eNOS-knockout mice compared with wild-type mice, despite that there were no statistically significant differences in microvascular parameters such as vessel diameter, blood velocity, volumetric flow rate, or

functional capillary density. Because the calculated longitudinal loss of O_2 down the length of arterioles was approximately 40% higher in eNOS-knockout mice compared with wild-type mice, Cabrales et al.[200] concluded that eNOS-knockout mice had greater O_2 extraction because of higher O_2 consumption in the surrounding tissue compared with wild-type mice.

Shibata et al.[201–203] conducted similar O_2 phosphorescence measurements in the microcirculation of rat cremaster muscle and quantified transmural O_2 gradients to evaluate changes in vascular wall O_2 consumption under different conditions, including inhibition of NOS activity with L-NAME. They concluded that there was an increase in vascular wall O_2 consumption after inhibiting NOS.[202,203] However, they attributed this finding to an increase in the workload for smooth muscle in the vasoconstricted vascular wall and not to the loss of the inhibitory effect of NO on O_2 consumption. They also reported that maximal vasodilation by papaverine decreased vascular wall O_2 consumption, which they attributed to a decrease in the smooth muscle workload.[201] However, another possibility is that there might have been greater NO production with an increase in WSS as blood flow increased during vasodilation, and the resulting increase in tissue NO inhibited O_2 consumption in the surrounding skeletal muscle. A possible difference in vascular wall workload does not seem to account for the apparently lower O_2 consumption rates in eNOS-knockout mice.[200] Because arterial blood pressure was higher in eNOS-knockout mice, vascular wall mechanical strain would be greater with a higher rate of vascular wall O_2 consumption than for the wild-type mice.

IV.D. O_2-dependent Consumption of Nitric Oxide

An in vitro electrode study of NO diffusion across strips of rat thoracic aorta reported that NO consumption in vascular tissue is first order with NO and first order with O_2, with an overall reaction = $k_1[NO][O_2]$, with k_1 determined experimentally to be 4×10^3 M^{-1} s^{-1}.[204] This is a much higher NO consumption rate than for direct auto-oxidation, which is first order with O_2 and second order with respect to NO.[205,206] At low O_2 concentrations in the bath, a 5-fold higher NO flux across the wall was found compared with NO flux when the bath O_2 concentration was high.[204] Thus, there is a possibility that some of the increase in NO measured during hypoxia might be attributed to a reduction in NO consumption. Vascular wall NO consumption may be related to the reaction between NO and cytochrome *c* oxidase. Alternately, it has been shown that the heme-containing protein cytoglobin, which is expressed in smooth muscle cells and adventitial fibroblasts, may act as an NO dioxygenase that consumes NO.[207] These in vitro studies, using murine fibroblasts, found that NO was mostly converted to NO_3^-, with very little formation of NO_2^-. NO also can be consumed and primarily converted to NO_2^- by several different oxygenases.[208–210]

V. RED BLOOD CELLS AS TARGETS OF NITRIC OXIDE

The prevailing viewpoint has been that RBCs are extremely strong sinks for NO. The possibility that some NO scavenged by Hb in the bloodstream could be recycled for downstream release is an attractive concept that has generated considerable interest and sometimes vigorous debate. However, a major challenge to this hypothesis is to explain how NO formed by the RBCs could be released without first reacting with concentrated Hb inside the RBCs. Azizi et al.[211] used the analogy that the RBC is a “black hole” for NO (i.e., it can enter but cannot get out). Also, ceruloplasmin in blood plasma catalyzes the conversion of NO to NO_2^-.[212] However, chemiluminescence measurements of NO in the headspace above a suspension of RBCs during deoxygenation suggest that either freely diffusible NO was released or another intermediate species escaped RBCs and was released from the blood as NO.[213] There have been a number of proposed mechanisms, and there is evidence that NO or possibly other vasoactive substances that are regulated by NO may be released by RBCs.

V.A. S-Nitrosylated Hemoglobin

Hypoxic vasodilation has been attributed to S-nitrosylated (SNO) Hb,[214] although this has been questioned.[215] Furthermore, a mathematical model of this mechanism by Chen et al.[216] predicts that very little, if any, NO can escape the RBCs and reach the vascular wall. Though the relative numbers of SNO-Hb molecules in the RBCs may be small, there is experimental evidence for their role in regulating hypoxic vasodilation. It has been shown that SNO-Hb in freshly drawn human blood falls below 20% of initial values within 3 hours, with additional bioassays indicating that hypoxic vasodilation is impaired.[217] Another study found similar decreases in SNO-Hb in banked human blood, falling to 30% after 1 day and to 17% after 1 week of storage.[218] Evidence was presented that hypoxic vasodilation can be restored by renitrosylation, based on measurements of increased coronary blood flow in dogs receiving renitrosylated blood compared with infusions of SNO-Hb–depleted blood. There are ongoing research efforts to investigate whether depletion of NO bioactivity is a type of storage lesion in banked blood that might account for adverse outcomes that are seen after blood transfusion in some higher risk populations.

V.B. Red Blood Cell Membrane eNOS

There was early evidence that eNOS is expressed in the RBC membrane,[219] although later studies concluded that the enzyme was not active.[220]. More recently, evidence has been reported that human RBCs express an active eNOS in the RBC membrane, which seems to be involved in the regulation of RBC deformability.[221] An in vitro study reported electrode measurements of NO in human blood under oxygenated (pO_2 approximately 150 mm Hg) or hypoxic (pO_2 approximately 36 mm Hg) conditions and found an increase in NO with shear only in hypoxic blood.[222] The NO response to shear could be blocked with L-NAME, which may be evidence that the NO was derived from RBC eNOS. Changes in RBC deformability in stored human blood have been reported to be much more gradual than changes in SNO-Hb.[217]

V.C. Nitrite as a Source of Nitric Oxide

1. In Blood—A role for NO_2^- in hypoxic vasodilation has received attention recently.[223,224] Based on comparative studies of NO_2^- uptake by RBCs from 4 different species, it seems that the main mechanisms for NO_2^- transport across the RBC membrane are passive diffusion of nitrous acid (HNO_2) and facilitated transport mediated via anion exchanger-1,[225] allowing accumulation of NO_2^- in the RBCs. In human RBCs, NO_2^- is approximately 300 nM—2 times higher than in blood plasma.[226] Also, there is an arterial to venous NO_2^- gradient in the bloodstream, from 176 nM in arterial blood decreasing to 143 nM in venous blood.[226] It has been known for several decades that Hb in the RBCs can reduce NO_2^- to NO.[227] More recently, is has been shown that the reaction is maximal around the P_{50} of the oxyhemoglobin saturation curve.[228] The NO reductase activity of Hb may be able to release NO from RBCs as they pass through the microcirculation and are deoxygenated, especially under hypoxic conditions.[223] As an alternative vasoactive species, it has been proposed that a NO_2^- reductase/anhydrase redox cycle in the RBCs catalyzes anaerobic conversion of 2 NO_2^- molecules into dinitrogen trioxide (N_2O_3), an uncharged molecule that presumably is not scavenged by Hb.[229] However, it is not clear whether N_2O_3 is vasoactive or converted to free NO in the vascular wall by other pathways.

Chen et al.[230] also modeled NO_2^- reduction by Hb and predicted that vascular wall NO could be increased only by picomolar levels at best. It was necessary to propose NO-protective mechanisms (facilitated transport from the RBCs or an intermediate species that is not scavenged by Hb) as possible ways to increase NO transport from the RBCs to the vascular wall.

2. In Tissue—Alternately, enzymes in tissues may provide another pathway for recovering NO from NO_2^-. NO produced by this mechanism would not be affected as strongly by Hb scavenging because the NO source would be much farther from the bloodstream. Recent evidence strongly suggests that tissues play a greater role than blood in reducing NO_2^- to NO when O_2 availability is limited under ischemic or hypoxic conditions. Feelisch et al.[231] reported a 3- to 5-fold lower rate for NO formation from NO_2^- reductase activity in RBCs compared with NO formation from tissue homogenates. Li et al.[232] reported that maximum NO production from anoxic RBCs is only 0.004 nM s^{-1} compared with rates >0.5 nM s^{-1} for anoxic heart and liver tissue homogenates. There is also in vitro evidence that sGC or other heme-proteins in vascular tissue can catalyze the reduction of NO_2^- to NO under aerobic conditions.[233]Buerk et al.[234] developed a diffusion and convection model for NO and O_2 transport in an arteriole that includes nitrite reductase activity in blood and in tissue. Compared with simulations without nitrite reductase activity, the model predicts that only very small amounts of additional NO in the vascular wall (pM increases) can result from nitrite reductase activity in RBCs, whereas much larger additional amounts of NO (nM increases) can be generated by tissue nitrite reductases, depending on tissue pO_2 levels. Varying blood flow or arterial blood pO_2 in the model was examined for effects on NO profiles in blood and tissue around the arteriole, showing a larger increase in additional NO caused by nitrite reductase activity in tissue for more hypoxic conditions.

V.D. Nitric Oxide–Mediated Adenosine Triphosphate Release

It has been shown that RBCs release ATP in response to decreased O_2, more acidic pH, and mechanical deformation[235–237] and that NO inhibits ATP release from RBCs.[238] More recently, it has been shown from studies with human RBCs that NO_2^- stimulates ATP release from human RBCs.[239] Another recent study in rats is consistent with this mechanism, suggesting that ATP released from RBCs was responsible for the decrease in mean arterial blood pressure after infusion with NO_2^--treated RBCs.[240] In this study, infusing 10 μM/kg NO_2^- caused an almost 2-fold increase in blood plasma ATP (from 4.8 to 9.1 nM) and a drop in blood pressure. Furthermore, injections of ATP in this range caused similar reductions in blood pressure. An increase in the releasable pool of ATP in the RBCs does not seem to be mediated by NO generated by NO_2^- reductase activity but is caused by the reaction between NO_2^- and Hb, so there is no requirement for NO to escape from the RBCs with this mechanism. However, ATP released from the RBCs can increase vascular wall NO bioavailability by increasing eNOS activity. A recent study of human umbilical vein ECs suggests NO production by eNOS is stimulated by ATP through P_2 purinergic receptors through a specific isoform of PKC, causing an increase in $[Ca^{2+}]_i$.[241] The requirement for O_2 to produce NO has not been included explicitly in many mathematical models of NO transport. Also, the physiologic status of the circulatory system to provide adequate tissue oxygenation can be uncertain in animal experiments, possibly confounding measurements and interpretation of various maneuvers that change NO production. Additional research is needed to gain a better understanding of the different mechanisms that have been outlined in this section.

VI. CONCLUSION

Future advances in understanding the role of NO in regulating blood flow at the level of the microcirculation will, without doubt, require both mathematical modeling and experimental investigation. Specific mechanisms for shear stress–dependent activation of NO production from different sources and complete characterization of NO losses from other reactions will need to be incorporated into more elaborate NO transport models. Models employing more complex geometries will need to be developed that better represent actual microcirculatory networks in different organs. Communication between EC and SMC through multiple types

of ion channels that regulate $[Ca^{2+}]_i$ will need to be incorporated. A better understanding of how endothelium-derived hyperpolarizing factors and NO interact through shared caveolin regulatory mechanisms is needed. Another fertile area of investigation is to understand how the posttranslational protein *S*-nitrosylation affects signaling pathways that are involved in regulating multiple physiologic processes. We have limited our review of pathological states, but it is evident that, as new modeling approaches are developed, there will be more work on predicting how NO either contributes to or helps to prevent pathologic changes. Though validating these theoretical models may prove to be challenging, further work should be encouraged because these model predictions will be invaluable for assessing normal physiological mechanisms as well as pathologic processes.

Acknowledgments

Supported in part by HL 068164 from NIH and CBET 0730547 from NSF.

REFERENCES

1. Murad F, Barber R. A hypothesis about cellular signaling with nitric oxide in the earliest life forms in evolution. Free Radic Biol Med. 2009; 47(9):1325–7. [PubMed: 19439177]
2. Ignarro LJ, Buga GM, Wood KS, Byrns RE, Chaudhuri G. Endothelium-derived relaxing factor produced and released from artery and vein is nitric oxide. Proc Natl Acad Sci U S A. 1987; 84(24): 9265–9. [PubMed: 2827174]
3. Palmer RM, Ferrige AG, Moncada S. Nitric oxide release accounts for the biological activity of endothelium-derived relaxing factor. Nature. 1987; 327(6122):524–6. [PubMed: 3495737]
4. Wink DA, Hanbauer I, Grisham MB, Laval F, Nims RW, Laval J, et al. Chemical biology of nitric oxide: regulation and protective and toxic mechanisms. Curr Top Cell Regul. 1996; 34:159–87. [PubMed: 8646847]
5. Thomas DD, Ridnour LA, Isenberg JS, Flores-Santana W, Switzer CH, Donzelli S, et al. The chemical biology of nitric oxide: implications in cellular signaling. Free Radic Biol Med. 2008; 45(1):18–31. [PubMed: 18439435]
6. Hall CN, Garthwaite J. What is the real physiological NO concentration in vivo? Nitric Oxide. 2009; 21(2):92–103. [PubMed: 19602444]
7. Lancaster JR Jr. Nitroxidative, nitrosative, and nitrative stress: kinetic predictions of reactive nitrogen species chemistry under biological conditions. Chem Res Toxicol. 2006; 19(9):1160–74. [PubMed: 16978020]
8. Huynh NN, Chin-Dusting J. Amino acids, arginase and nitric oxide in vascular health. Clin Exp Pharmacol Physiol. 2006; 33(1-2):1–8. [PubMed: 16445692]
9. Moens AL, Kass DA. Tetrahydrobiopterin and cardiovascular disease. Arterioscler Thromb Vasc Biol. 2006; 26(11):2439–44. [PubMed: 16946131]
10. Napoli C, de Nigris F, Williams-Ignarro S, Pignalosa O, Sica V, Ignarro LJ. Nitric oxide and atherosclerosis: an update. Nitric Oxide. 2006; 15(4):265–79. [PubMed: 16684613]
11. Morris SM Jr. Recent advances in arginine metabolism: roles and regulation of the arginases. Br J Pharmacol. 2009; 157(6):922–30. [PubMed: 19508396]
12. Berkowitz DE, White R, Li D, Minhas KM, Cernetich A, Kim S, et al. Arginase reciprocally regulates nitric oxide synthase activity and contributes to endothelial dysfunction in aging blood vessels. Circulation. 2003; 108(16):2000–6. [PubMed: 14517171]
13. Santhanam L, Christianson DW, Nyhan D, Berkowitz DE. Arginase and vascular aging. J Appl Physiol. 2008; 105(5):1632–42. [PubMed: 18719233]
14. Kim JH, Bugaj LJ, Oh YJ, Bivalacqua TJ, Ryoo S, Soucy KG, et al. Arginase inhibition restores NOS coupling and reverses endothelial dysfunction and vascular stiffness in old rats. J Appl Physiol. 2009; 107(4):1249–57. [PubMed: 19661445]
15. Tsikas D, Boger RH, Sandmann J, Bode-Boger SM, Frolich JC. Endogenous nitric oxide synthase inhibitors are responsible for the L-arginine paradox. FEBS Lett. 2000; 478(1-2):1–3. [PubMed: 10922458]

16. Zoccali C. Asymmetric dimethylarginine (ADMA): a cardiovascular and renal risk factor on the move. J Hypertens. 2006; 24(4):611–9. [PubMed: 16531785]
17. Mittermayer F, Krzyzanowska K, Exner M, Mlekusch W, Amighi J, Sabeti S, et al. Asymmetric dimethylarginine predicts major adverse cardiovascular events in patients with advanced peripheral artery disease. Arterioscler Thromb Vasc Biol. 2006; 26(11):2536–40. [PubMed: 16931791]
18. Boger RH. Asymmetric dimethylarginine (ADMA) and cardiovascular disease: insights from prospective clinical trials. Vasc Med. 2005; 10(Suppl 1):S19–25. [PubMed: 16444865]
19. Ando J, Yamamoto K. Vascular mechanobiology: endothelial cell responses to fluid shear stress. Circ J. 2009; 73(11):1983–92. [PubMed: 19801852]
20. Kwan HY, Leung PC, Huang Y, Yao X. Depletion of intracellular Ca^{2+} stores sensitizes the flow-induced Ca^{2+} influx in rat endothelial cells. Circ Res. 2003; 92(3):286–92. [PubMed: 12595340]
21. Tanaka H, Takamatsu T. Calcium spots: elementary signals in response to mechanical stress in vascular endothelial cells. Circ Res. 2001; 88(9):852–4. [PubMed: 11348991]
22. Hong D, Jaron D, Buerk DG, Barbee KA. Heterogeneous response of microvascular endothelial cells to shear stress. Am J Physiol Heart Circ Physiol. 2006; 290(6):H2498–508. [PubMed: 16415079]
23. Kumagai R, Lu X, Kassab GS. Role of glycocalyx in flow-induced production of nitric oxide and reactive oxygen species. Free Radic Biol Med. 2009; 47(5):600–7. [PubMed: 19500664]
24. Nauli SM, Kawanabe Y, Kaminski JJ, Pearce WJ, Ingber DE, Zhou J. Endothelial cilia are fluid shear sensors that regulate calcium signaling and nitric oxide production through polycystin-1. Circulation. 2008; 117(9):1161–71. [PubMed: 18285569]
25. AbouAlaiwi WA, Takahashi M, Mell BR, Jones TJ, Ratnam S, Kolb RJ, et al. Ciliary polycystin-2 is a mechanosensitive calcium channel involved in nitric oxide signaling cascades. Circ Res. 2009; 104(7):860–9. [PubMed: 19265036]
26. Mendoza SA, Fang J, Gutterman DD, Wilcox DA, Bubolz AH, Li R, et al. TRPV4-mediated endothelial Ca^{2+} influx and vasodilation in response to shear stress. Am J Physiol Heart Circ Physiol. 2010; 298(2):H466–76. [PubMed: 19966050]
27. Rizzo V, McIntosh DP, Oh P, Schnitzer JE. In situ flow activates endothelial nitric oxide synthase in luminal caveolae of endothelium with rapid caveolin dissociation and calmodulin association. J Biol Chem. 1998; 273(52):34724–9. [PubMed: 9856995]
28. Dimmeler S, Fleming I, Fisslthaler B, Hermann C, Busse R, Zeiher AM. Activation of nitric oxide synthase in endothelial cells by Akt-dependent phosphorylation. Nature. 1999; 399(6736):601–5. [PubMed: 10376603]
29. Jin ZG, Ueba H, Tanimoto T, Lungu AO, Frame MD, Berk BC. Ligand-independent activation of vascular endothelial growth factor receptor 2 by fluid shear stress regulates activation of endothelial nitric oxide synthase. Circ Res. 2003; 93(4):354–63. [PubMed: 12893742]
30. Fleming I, Fisslthaler B, Dixit M, Busse R. Role of PECAM-1 in the shear-stress-induced activation of Akt and the endothelial nitric oxide synthase (eNOS) in endothelial cells. J Cell Sci. 2005; 118(Pt 18):4103–11. [PubMed: 16118242]
31. Loufrani L, Retailleau K, Bocquet A, Dumont O, Danker K, Louis H, et al. Key role of alpha(1)beta(1)-integrin in the activation of PI3-kinase-Akt by flow (shear stress) in resistance arteries. Am J Physiol Heart Circ Physiol. 2008; 294(4):H1906–13. [PubMed: 18245559]
32. Hong D, Jaron D, Buerk DG, Barbee KA. Transport-dependent calcium signaling in spatially segregated cellular caveolar domains. Am J Physiol Cell Physiol. 2008; 294(3):C856–66. [PubMed: 18160488]
33. Barbee KA, Mundel T, Lal R, Davies PF. Subcellular distribution of shear stress at the surface of flow-aligned and nonaligned endothelial monolayers. Am J Physiol. 1995; 268(4 Pt 2):H1765–72. [PubMed: 7733381]
34. Tsoukias NM. Calcium dynamics and signaling in vascular regulation: computational models. Wiley Interdiscip Rev Syst Biol Med. 2011; 3(1):93–106. [PubMed: 21061306]
35. Wiesner TF, Berk BC, Nerem RM. A mathematical model of cytosolic calcium dynamics in human umbilical vein endothelial cells. Am J Physiol. 1996; 270(5 Pt 1):C1556–69. [PubMed: 8967458]

36. Wiesner TF, Berk BC, Nerem RM. A mathematical model of the cytosolic-free calcium response in endothelial cells to fluid shear stress. Proc Natl Acad Sci U S A. 1997; 94(8):3726–31. [PubMed: 9108045]
37. Wong AY, Klassen GA. A model of electrical activity and cytosolic calcium dynamics in vascular endothelial cells in response to fluid shear stress. Ann Biomed Eng. 1995; 23(6):822–32. [PubMed: 8572432]
38. Schuster A, Beny JL, Meister JJ. Modeling the electrophysiological endothelial cell response to bradykinin. Eur Biophys J. 2003; 32(4):370–80. [PubMed: 12851795]
39. Silva HS, Kapela A, Tsoukias NM. A mathematical model of plasma membrane electrophysiology and calcium dynamics in vascular endothelial cells. Am J Physiol Cell Physiol. 2007; 293(1):C277–93. [PubMed: 17459942]
40. Plank MJ, Wall DJ, David T. Atherosclerosis and calcium signaling in endothelial cells. Prog Biophys Mol Biol. 2006; 91(3):287–313. [PubMed: 16171849]
41. Fleming I, Busse R. Molecular mechanisms involved in the regulation of the endothelial nitric oxide synthase. Am J Physiol Regul Integr Comp Physiol. 2003; 284(1):R1–12. [PubMed: 12482742]
42. Fleming I, Busse R. Signal transduction of eNOS activation. Cardiovasc Res. 1999; 43(3):532–41. [PubMed: 10690325]
43. Ayajiki K, Kindermann M, Hecker M, Fleming I, Busse R. Intracellular pH and tyrosine phosphorylation but not calcium determine shear stress-induced nitric oxide production in native endothelial cells. Circ Res. 1996; 78(5):750–8. [PubMed: 8620594]
44. Qiu W, Kass DA, Hu Q, Ziegelstein RC. Determinants of shear stress-stimulated endothelial nitric oxide production assessed in real-time by 4,5-diaminofluorescein fluorescence. Biochem Biophys Res Commun. 2001; 286(2):328–35. [PubMed: 11500041]
45. Kuchan MJ, Frangos JA. Role of calcium and calmodulin in flow-induced nitric oxide production in endothelial cells. Am J Physiol. 1994; 266(3 Pt 1):C628–36. [PubMed: 8166225]
46. Garcia-Cardena G, Oh P, Liu J, Schnitzer JE, Sessa WC. Targeting of nitric oxide synthase to endothelial cell caveolae via palmitoylation: implications for nitric oxide signaling. Proc Natl Acad Sci U S A. 1996; 93(13):6448–53. [PubMed: 8692835]
47. Plank MJ, Wall DJ, David T. The role of endothelial calcium and nitric oxide in the localisation of atherosclerosis. Math Biosci. 2007; 207(1):26–39. [PubMed: 17070868]
48. Cheng C, van Haperen R, de Waard M, van Damme LC, Tempel D, Hanemaaijer L, et al. Shear stress affects the intracellular distribution of eNOS: direct demonstration by a novel in vivo technique. Blood. 2005; 106(12):3691–8. [PubMed: 16105973]
49. Comerford A, Plank MJ, David T. Endothelial nitric oxide synthase and calcium production in arterial geometries: an integrated fluid mechanics/cell model. J Biomech Eng. 2008; 130(1): 011010–1-13. [PubMed: 18298186]
50. Munaron L. A tridimensional model of proangiogenic calcium signals in endothelial cells. Open Biol J. 2009; 2:114–29.
51. Tomatis C, Fiorio Pla A, Munaron L. Cytosolic calcium microdomains by arachidonic acid and nitric oxide in endothelial cells. Cell Calcium. 2007; 41(3):261–9. [PubMed: 16920190]
52. Huang B, Chen SC, Wang DL. Shear flow increases S-nitrosylation of proteins in endothelial cells. Cardiovasc Res. 2009; 83(3):536–46. [PubMed: 19447776]
53. Grumbach IM, Chen W, Mertens SA, Harrison DG. A negative feedback mechanism involving nitric oxide and nuclear factor kappa-B modulates endothelial nitric oxide synthase transcription. J Mol Cell Cardiol. 2005; 39(4):595–603. [PubMed: 16099468]
54. Li Y, Zheng J, Bird IM, Magness RR. Effects of pulsatile shear stress on signaling mechanisms controlling nitric oxide production, endothelial nitric oxide synthase phosphorylation, and expression in ovine fetoplacental artery endothelial cells. Endothelium. 2005; 12(1-2):21–39. [PubMed: 16036314]
55. Kanai AJ, Strauss HC, Truskey GA, Crews AL, Grunfeld S, Malinski T. Shear stress induces ATP-independent transient nitric oxide release from vascular endothelial cells, measured directly with a porphyrinic microsensor. Circ Res. 1995; 77(2):284–93. [PubMed: 7614715]

56. Fadel AA, Barbee KA, Jaron D. A computational model of nitric oxide production and transport in a parallel plate flow chamber. Ann Biomed Eng. 2009; 37(5):943–54. [PubMed: 19242805]
57. Plata AM, Sherwin SJ, Krams R. Endothelial nitric oxide production and transport in flow chambers: the importance of convection. Ann Biomed Eng. 2010; 38:2805–16. [PubMed: 20390451]
58. Cheng C, Tempel D, Oostlander A, Helderman F, Gijsen F, Wentzel J, et al. Rapamycin modulates the eNOS vs. shear stress relationship. Cardiovasc Res. 2008; 78(1):123–9. [PubMed: 18079107]
59. Andrews AM, Jaron D, Buerk DG, Kirby PL, Barbee KA. Direct, real-time measurement of shear stress-induced nitric oxide produced from endothelial cells in vitro. Nitric Oxide. 2010; 23(4):335–42. [PubMed: 20719252]
60. Cornelissen AJ, Dankelman J, VanBavel E, Spaan JA. Balance between myogenic, flow-dependent, and metabolic flow control in coronary arterial tree: a model study. Am J Physiol Heart Circ Physiol. 2002; 282(6):H2224–37. [PubMed: 12003832]
61. Kuo L, Davis MJ, Chilian WM. Longitudinal gradients for endothelium-dependent and -independent vascular responses in the coronary microcirculation. Circulation. 1995; 92(3):518–25. [PubMed: 7543382]
62. Liao JC, Kuo L. Interaction between adenosine and flow-induced dilation in coronary microvascular network. Am J Physiol. 1997; 272(4 Pt 2):H1571–81. [PubMed: 9139938]
63. Kapela A, Bezerianos A, Tsoukias NM. A mathematical model of Ca^{2+} dynamics in rat mesenteric smooth muscle cell: agonist and NO stimulation. J Theor Biol. 2008; 253(2):238–60. [PubMed: 18423672]
64. Kapela A, Nagaraja S, Tsoukias NM. A mathematical model of vasoreactivity in rat mesenteric arterioles. II. Conducted vasoreactivity. Am J Physiol Heart Circ Physiol. 2010; 298:H52–65. [PubMed: 19855062]
65. Kapela A, Bezerianos A, Tsoukias NM. A mathematical model of vasoreactivity in rat mesenteric arterioles. I. Myoendothelial communication. Microcirculation. 2009; 16(8):694–713. [PubMed: 19905969]
66. Segal SS. Cell-to-cell communication coordinates blood flow control. Hypertension. 1994; 23(6 Pt 2):1113–20. [PubMed: 8206602]
67. Segal SS, Duling BR. Flow control among microvessels coordinated by intercellular conduction. Science. 1986; 234(4778):868–70. [PubMed: 3775368]
68. Segal SS, Damon DN, Duling BR. Propagation of vasomotor responses coordinates arteriolar resistances. Am J Physiol. 1989; 256(3 Pt 2):H832–7. [PubMed: 2923241]
69. Uhrenholt TR, Domeier TL, Segal SS. Propagation of calcium waves along endothelium of hamster feed arteries. Am J Physiol Heart Circ Physiol. 2007; 292(3):H1634–40. [PubMed: 17098832]
70. Uhrenholt TR, Schjerning J, Vanhoutte PM, Jensen BL, Skott O. Intercellular calcium signaling and nitric oxide feedback during constriction of rabbit renal afferent arterioles. Am J Physiol Renal Physiol. 2007; 292(4):F1124–31. [PubMed: 17148782]
71. Figueroa XF, Chen CC, Campbell KP, Damon DN, Day KH, Ramos S, et al. Are voltage-dependent ion channels involved in the endothelial cell control of vasomotor tone? Am J Physiol Heart Circ Physiol. 2007; 293(3):H1371–83. [PubMed: 17513486]
72. de Wit C. Different pathways with distinct properties conduct dilations in the microcirculation in vivo. Cardiovasc Res. 2010; 85(3):604–13. [PubMed: 19820254]
73. Ngo AT, Jensen LJ, Riemann M, Holstein-Rathlou NH, Torp-Pedersen C. Oxygen sensing and conducted vasomotor responses in mouse cremaster arterioles in situ. Pflugers Arch. 2010; 460(1): 41–53. [PubMed: 20383716]
74. Riemann M, Rai A, Ngo AT, Dziegiel MH, Holstein-Rathlou NH, Torp-Pedersen C. Oxygen-dependent vasomotor responses are conducted upstream in the mouse cremaster microcirculation. J Vasc Res. 2011; 48(1):79–89. [PubMed: 20639650]
75. Denninger JW, Marletta MA. Guanylate cyclase and the ·NO/cGMP signaling pathway. Biochim Biophys Acta. 1999; 1411(2-3):334–50. [PubMed: 10320667]

76. Zhao Y, Brandish PE, Ballou DP, Marletta MA. A molecular basis for nitric oxide sensing by soluble guanylate cyclase. Proc Natl Acad Sci U S A. 1999; 96(26):14753–8. [PubMed: 10611285]
77. Roy B, Halvey EJ, Garthwaite J. An enzyme-linked receptor mechanism for nitric oxide-activated guanylyl cyclase. J Biol Chem. 2008; 283(27):18841–51. [PubMed: 18463095]
78. Ballou DP, Zhao Y, Brandish PE, Marletta MA. Revisiting the kinetics of nitric oxide (NO) binding to soluble guanylate cyclase: the simple NO-binding model is incorrect. Proc Natl Acad Sci U S A. 2002; 99(19):12097–101. [PubMed: 12209005]
79. Condorelli P, George SC. In vivo control of soluble guanylate cyclase activation by nitric oxide: a kinetic analysis. Biophys J. 2001; 80(5):2110–9. [PubMed: 11325714]
80. Russwurm M, Behrends S, Harteneck C, Koesling D. Functional properties of a naturally occurring isoform of soluble guanylyl cyclase. Biochem J. 1998; 335(Pt 1):125–30. [PubMed: 9742221]
81. Stone JR, Marletta MA. Spectral and kinetic studies on the activation of soluble guanylate cyclase by nitric oxide. Biochemistry. 1996; 35(4):1093–9. [PubMed: 8573563]
82. Cary SP, Winger JA, Derbyshire ER, Marletta MA. Nitric oxide signaling: no longer simply on or off. Trends Biochem Sci. 2006; 31(4):231–9. [PubMed: 16530415]
83. Yang J, Clark JW, Bryan RM, Robertson CS. Mathematical modeling of the nitric oxide/cGMP pathway in the vascular smooth muscle cell. Am J Physiol Heart Circ Physiol. 2005; 289(2):H886–97. [PubMed: 15833804]
84. Suzuki T, Suematsu M, Makino R. Organic phosphates as a new class of soluble guanylate cyclase inhibitors. FEBS Lett. 2001; 507(1):49–53. [PubMed: 11682058]
85. Ruiz-Stewart I, Tiyyagura SR, Lin JE, Kazerounian S, Pitari GM, Schulz S, et al. Guanylyl cyclase is an ATP sensor coupling nitric oxide signaling to cell metabolism. Proc Natl Acad Sci U S A. 2004; 101(1):37–42. [PubMed: 14684830]
86. Garthwaite J. New insight into the functioning of nitric oxide-receptive guanylyl cyclase: physiological and pharmacological implications. Mol Cell Biochem. 2010; 334(1-2):221–32. [PubMed: 20012469]
87. Tsoukias NM. Nitric oxide bioavailability in the microcirculation: insights from mathematical models. Microcirculation. 2008; 15(8):813–34. [PubMed: 18608992]
88. Buerk DG. Can we model nitric oxide biotransport? A survey of mathematical models for a simple diatomic molecule with surprisingly complex biological activities. Annu Rev Biomed Eng. 2001; 3:109–43. [PubMed: 11447059]
89. Butler AR, Megson IL, Wright PG. Diffusion of nitric oxide and scavenging by blood in the vasculature. Biochim Biophys Acta. 1998; 1425(1):168–76. [PubMed: 9813307]
90. Liao JC, Hein TW, Vaughn MW, Huang KT, Kuo L. Intravascular flow decreases erythrocyte consumption of nitric oxide. Proc Natl Acad Sci U S A. 1999; 96(15):8757–61. [PubMed: 10411948]
91. Vaughn MW, Kuo L, Liao JC. Effective diffusion distance of nitric oxide in the microcirculation. Am J Physiol. 1998; 274(5 Pt 2):H1705–H14. [PubMed: 9612383]
92. Vaughn MW, Huang KT, Kuo L, Liao JC. Erythrocytes possess an intrinsic barrier to nitric oxide consumption. J Biol Chem. 2000; 275(4):2342–8. [PubMed: 10644684]
93. Lancaster JR Jr. Simulation of the diffusion and reaction of endogenously produced nitric oxide. Proc Natl Acad Sci U S A. 1994; 91(17):8137–41. [PubMed: 8058769]
94. Lancaster JR Jr. A tutorial on the diffusibility and reactivity of free nitric oxide. Nitric Oxide. 1997; 1(1):18–30. [PubMed: 9701041]
95. Chen X, Jaron D, Barbee KA, Buerk DG. The influence of radial RBC distribution, blood velocity profiles, and glycocalyx on coupled NO/O_2 transport. J Appl Physiol. 2006; 100(2):482–92. [PubMed: 16210436]
96. Lamkin-Kennard KA, Jaron D, Buerk DG. Impact of the Fahraeus effect on NO and O_2 biotransport: a computer model. Microcirculation. 2004; 11(4):337–49. [PubMed: 15280073]
97. Lamkin-Kennard K, Jaron D, Buerk DG. Modeling the regulation of oxygen consumption by nitric oxide. Adv Exp Med Biol. 2003; 510:145–9. [PubMed: 12580419]

98. Chen X, Buerk DG, Barbee KA, Jaron D. A model of NO/O_2 transport in capillary-perfused tissue containing an arteriole and venule pair. Ann Biomed Eng. 2007; 35(4):517–29. [PubMed: 17235703]
99. Kavdia M, Tsoukias NM, Popel AS. Model of nitric oxide diffusion in an arteriole: impact of hemoglobin-based blood substitutes. Am J Physiol Heart Circ Physiol. 2002; 282(6):H2245–53. [PubMed: 12003834]
100. El-Farra NH, Christofides PD, Liao JC. Analysis of nitric oxide consumption by erythrocytes in blood vessels using a distributed multicellular model. Ann Biomed Eng. 2003; 31(3):294–309. [PubMed: 12680727]
101. Buerk DG, Lamkin-Kennard K, Jaron D. Modeling the influence of superoxide dismutase on superoxide and nitric oxide interactions, including reversible inhibition of oxygen consumption. Free Radic Biol Med. 2003; 34(11):1488–503. [PubMed: 12757859]
102. Lamkin-Kennard KA, Buerk DG, Jaron D. Interactions between NO and O_2 in the microcirculation: a mathematical analysis. Microvasc Res. 2004; 68(1):38–50. [PubMed: 15219419]
103. Smith KM, Moore LC, Layton HE. Advective transport of nitric oxide in a mathematical model of the afferent arteriole. Am J Physiol Renal Physiol. 2003; 284(5):F1080–96. [PubMed: 12712988]
104. Lu X, Kassab GS. Nitric oxide is significantly reduced in ex vivo porcine arteries during reverse flow because of increased superoxide production. J Physiol. 2004; 561(Pt 2):575–82. [PubMed: 15579542]
105. Chen K, Popel AS. Theoretical analysis of biochemical pathways of nitric oxide release from vascular endothelial cells. Free Radic Biol Med. 2006; 41(4):668–80. [PubMed: 16864000]
106. Vaughn MW, Kuo L, Liao JC. Estimation of nitric oxide production and reaction rates in tissue by use of a mathematical model. Am J Physiol. 1998; 274(6 Pt 2):H2163–76. [PubMed: 9841542]
107. Malinski T, Taha Z, Grunfeld S, Patton S, Kapturczak M, Tomboulian P. Diffusion of nitric oxide in the aorta wall monitored in situ by porphyrinic microsensors. Biochem Biophys Res Commun. 1993; 193(3):1076–82. [PubMed: 8323533]
108. Van Hove CE, Van der Donckt C, Herman AG, Bult H, Fransen P. Vasodilator efficacy of nitric oxide depends on mechanisms of intracellular calcium mobilization in mouse aortic smooth muscle cells. Br J Pharmacol. 2009; 158(3):920–30. [PubMed: 19788496]
109. Tsoukias NM, Kavdia M, Popel AS. A theoretical model of nitric oxide transport in arterioles: frequency- vs. amplitude-dependent control of cGMP formation. Am J Physiol Heart Circ Physiol. 2004; 286(3):H1043–56. [PubMed: 14592938]
110. Kavdia M, Popel AS. Wall shear stress differentially affects NO level in arterioles for volume expanders and Hb-based O_2 carriers. Microvasc Res. 2003; 66(1):49–58. [PubMed: 12826074]
111. Tsoukias NM, Popel AS. Erythrocyte consumption of nitric oxide in presence and absence of plasma-based hemoglobin. Am J Physiol Heart Circ Physiol. 2002; 282(6):H2265–77. [PubMed: 12003837]
112. Liu X, Samouilov A, Lancaster JR Jr. Zweier JL. Nitric oxide uptake by erythrocytes is primarily limited by extracellular diffusion not membrane resistance. J Biol Chem. 2002; 277(29):26194–9. [PubMed: 12006567]
113. Silverman TA, Weiskopf RB. Hemoglobin-based oxygen carriers: current status and future directions. Anesthesiology. 2009; 111(5):946–63. [PubMed: 19858869]
114. Kavdia M, Popel AS. Venular endothelium-derived NO can affect paired arteriole: a computational model. Am J Physiol Heart Circ Physiol. 2006; 290(2):H716–23. [PubMed: 16155098]
115. Kavdia M. A computational model for free radicals transport in the microcirculation. Antioxid Redox Signal. 2006; 8(7-8):1103–11. [PubMed: 16910758]
116. Buerk DG. Mathematical modeling of the interaction between oxygen, nitric oxide and superoxide. Adv Exp Med Biol. 2009; 645:7–12. [PubMed: 19227443]
117. Chen, X. Computational modeling the mechanisms of blood flow coupled nitric oxide transport [dissertation]. Drexel University; Philadelphia, PA: 2007.

118. Kashiwagi S, Kajimura M, Yoshimura Y, Suematsu M. Nonendothelial source of nitric oxide in arterioles but not venules. Alternative source revealed in vivo by diaminofluorescein microfluorography. Circ Res. 2002; 91:e55–e64. [PubMed: 12480826]
119. Nellore K, Harris NR. Nitric oxide measurements in rat mesentery reveal disrupted venulo-arteriolar communication in diabetes. Microcirculation. 2004; 11(5):415–23. [PubMed: 15280067]
120. Hiratsuka M, Katayama T, Uematsu K, Kiyomura M, Ito M. In vivo visualization of nitric oxide and interactions among platelets, leukocytes, and endothelium following hemorrhagic shock and reperfusion. Inflamm Res. 2009; 58(8):463–71. [PubMed: 19262990]
121. Zhang X, Kim WS, Hatcher N, Potgieter K, Moroz LL, Gillette R, et al. Interfering with nitric oxide measurements. 4,5-diaminofluorescein reacts with dehydroascorbic acid and ascorbic acid. J Biol Chem. 2002; 277(50):48472–8. [PubMed: 12370177]
122. Nagata N, Momose K, Ishida Y. Inhibitory effects of catecholamines and anti-oxidants on the fluorescence reaction of 4,5-diaminofluorescein, DAF-2, a novel indicator of nitric oxide. J Biochem. 1999; 125(4):658–61. [PubMed: 10101276]
123. Rodriguez J, Specian V, Maloney R, Jourd'heuil D, Feelisch M. Performance of diamino fluorophores for the localization of sources and targets of nitric oxide. Free Radic Biol Med. 2005; 38(3):356–68. [PubMed: 15629864]
124. Balcerczyk A, Soszynski M, Bartosz G. On the specificity of 4-amino-5-methylamino-2′,7′-difluorofluorescein as a probe for nitric oxide. Free Radic Biol Med. 2005; 39(3):327–35. [PubMed: 15993331]
125. Lacza Z, Horn TF, Snipes JA, Zhang J, Roychowdhury S, Horvath EM, et al. Lack of mitochondrial nitric oxide production in the mouse brain. J Neurochem. 2004; 90(4):942–51. [PubMed: 15287900]
126. Planchet E, Kaiser WM. Nitric oxide (NO) detection by DAF fluorescence and chemiluminescence: a comparison using abiotic and biotic NO sources. J Exp Bot. 2006; 57(12): 3043–55. [PubMed: 16893978]
127. Jourd'heuil D. Increased nitric oxide-dependent nitrosylation of 4,5-diaminofluorescein by oxidants: implications for the measurement of intracellular nitric oxide. Free Radic Biol Med. 2002; 33(5):676–84. [PubMed: 12208354]
128. Duran WN, Seyama A, Yoshimura K, Gonzalez DR, Jara PI, Figueroa XF, et al. Stimulation of NO production and of eNOS phosphorylation in the microcirculation in vivo. Microvasc Res. 2000; 60(2):104–11. [PubMed: 10964584]
129. Figueroa XF, Martinez AD, Gonzalez DR, Jara PI, Ayala S, Boric MP. In vivo assessment of microvascular nitric oxide production and its relation with blood flow. Am J Physiol Heart Circ Physiol. 2001; 280(3):H1222–31. [PubMed: 11179067]
130. Figueroa XF, Gonzalez DR, Martinez AD, Duran WN, Boric MP. ACh-induced endothelial NO synthase translocation, NO release and vasodilatation in the hamster microcirculation in vivo. J Physiol. 2002; 544(Pt 3):883–96. [PubMed: 12411531]
131. Bohlen HG. Mechanism of increased vessel wall nitric oxide concentrations during intestinal absorption. Am J Physiol. 1998; 275(2 Pt 2):H542–50. [PubMed: 9683443]
132. Vukosavljevic N, Jaron D, Barbee KA, Buerk DG. Quantifying the L-arginine paradox in vivo. Microvasc Res. 2006; 71(1):48–54. [PubMed: 16316668]
133. Nase GP, Tuttle J, Bohlen HG. Reduced perivascular PO_2 increases nitric oxide release from endothelial cells. Am J Physiol Heart Circ Physiol. 2003; 285(2):H507–15. [PubMed: 12860561]
134. Gerova M, Mesaros S, Kristek F, Kittova M, Malinski T. NO concentration in the periendothelial area of the femoral artery of the dog measured in vivo. Physiol Res. 1998; 47(3):169–75. [PubMed: 9803481]
135. Gerova M, Mesaros S, Kittova M, Hatrik S, Kristek F, Malinski T. Nitric oxide in the periendothelial area of femoral vein of the dog assessed in vivo by a porphyrinic sensor. Physiol Res. 1996; 45(4):285–9. [PubMed: 9085351]
136. Kim DD, Kanetaka T, Duran RG, Sanhez FA, Bohlen HG, Dura WN. Independent regulation of periarteriolar and perivenular nitric oxide mechanisms in the in vivo hamster cheek pouch microvasculature. Microcirculation. 2009; 16(4):323–30. [PubMed: 19235626]

137. Bohlen HG, Zhou X, Unthank JL, Miller SJ, Bills R. Transfer of nitric oxide by blood from upstream to downstream resistance vessels causes microvascular dilation. Am J Physiol Heart Circ Physiol. 2009; 297(4):H1337–46. [PubMed: 19666847]
138. Buerk DG. Nitric oxide regulation of microvascular oxygen. Antioxid Redox Signal. 2007; 9(7): 829–43. [PubMed: 17508909]
139. Azarov I, Huang KT, Basu S, Gladwin MT, Hogg N, Kim-Shapiro DB. Nitric oxide scavenging by red blood cells as a function of hematocrit and oxygenation. J Biol Chem. 2005; 280(47): 39024–32. [PubMed: 16186121]
140. Wagner L, Hoey JG, Erdely A, Boegehold MA, Baylis C. The nitric oxide pathway is amplified in venular vs arteriolar cultured rat mesenteric endothelial cells. Microvasc Res. 2001; 62(3): 401–9. [PubMed: 11678642]
141. Forstermann U, Closs EI, Pollock JS, Nakane M, Schwarz P, Gath I, et al. Nitric oxide synthase isozymes. Characterization, purification, molecular cloning, and functions. Hypertension. 1994; 23(6 Pt 2):1121–31. [PubMed: 7515853]
142. Bode-Boger SM, Scalera F, Ignarro LJ. The L-arginine paradox: Importance of the L-arginine/asymmetrical dimethylarginine ratio. Pharmacol Ther. 2007; 114(3):295–306. [PubMed: 17482266]
143. Pezzuto L, Bohlen HG. Extracellular arginine rapidly dilates in vivo intestinal arteries and arterioles through a nitric oxide mechanism. Microcirculation. 2008; 15(2):123–35. [PubMed: 18260003]
144. Zani BG, Bohlen HG. Transport of extracellular l-arginine via cationic amino acid transporter is required during in vivo endothelial nitric oxide production. Am J Physiol Heart Circ Physiol. 2005; 289(4):H1381–90. [PubMed: 15849232]
145. Joshi MS, Ferguson TB Jr, Johnson FK, Johnson RA, Parthasarathy S, Lancaster JR Jr. Receptor-mediated activation of nitric oxide synthesis by arginine in endothelial cells. Proc Natl Acad Sci U S A. 2007; 104(24):9982–7. [PubMed: 17535904]
146. Rengasamy A, Johns RA. Determination of K_m for oxygen of nitric oxide synthase isoforms. J Pharmacol Exp Ther. 1996; 276(1):30–3. [PubMed: 8558447]
147. Ostergaard L, Stankevicius E, Andersen MR, Eskildsen-Helmond Y, Ledet T, Mulvany MJ, et al. Diminished NO release in chronic hypoxic human endothelial cells. Am J Physiol Heart Circ Physiol. 2007; 293(5):H2894–903. [PubMed: 17720765]
148. Pohl U, Busse R. Hypoxia stimulates release of endothelium-derived relaxant factor. Am J Physiol. 1989; 256(6 Pt 2):H1595–600. [PubMed: 2660596]
149. Edmunds NJ, Marshall JM. The roles of nitric oxide in dilating proximal and terminal arterioles of skeletal muscle during systemic hypoxia. J Vasc Res. 2003; 40(1):68–76. [PubMed: 12644727]
150. Xiang L, Naik JS, Hester RL. Functional vasodilation in the rat spinotrapezius muscle: role of nitric oxide, prostanoids and epoxyeicosatrienoic acids. Clin Exp Pharmacol Physiol. 2008; 35(5-6):617–24. [PubMed: 18215183]
151. Bohlen HG. Protein kinase betaII in Zucker obese rats compromises oxygen and flow-mediated regulation of nitric oxide formation. Am J Physiol Heart Circ Physiol. 2004; 286(2):H492–7. [PubMed: 14715497]
152. Van Mil AH, Spilt A, Van Buchem MA, Bollen EL, Teppema L, Westendorp RG, et al. Nitric oxide mediates hypoxia-induced cerebral vasodilation in humans. J Appl Physiol. 2002; 92(3): 962–6. [PubMed: 11842027]
153. Hudetz AG, Shen H, Kampine JP. Nitric oxide from neuronal NOS plays critical role in cerebral capillary flow response to hypoxia. Am J Physiol. 1998; 274(3 Pt 2):H982–9. [PubMed: 9530212]
154. Bauser-Heaton HD, Bohlen HG. Cerebral microvascular dilation during hypotension and decreased oxygen tension: a role for nNOS. Am J Physiol Heart Circ Physiol. 2007; 293(4):H2193–201. [PubMed: 17630350]
155. Bauser-Heaton HD, Song J, Bohlen HG. Cerebral microvascular nNOS responds to lowered oxygen tension through a bumetanide-sensitive cotransporter and sodium-calcium exchanger. Am J Physiol Heart Circ Physiol. 2008; 294(5):H2166–73. [PubMed: 18326806]

156. Zani BG, Bohlen HG. Sodium channels are required during in vivo sodium chloride hyperosmolarity to stimulate increase in intestinal endothelial nitric oxide production. Am J Physiol Heart Circ Physiol. 2005; 288(1):H89–95. [PubMed: 15331363]

157. Pasgaard T, Stankevicius E, Jorgensen MM, Ostergaard L, Simonsen U, Frobert O. Hyperoxia reduces basal release of nitric oxide and contracts porcine coronary arteries. Acta Physiol (Oxf). 2007; 191(4):285–96. [PubMed: 17784906]

158. Thom SR, Fisher D, Zhang J, Bhopale VM, Ohnishi ST, Kotake Y, et al. Stimulation of perivascular nitric oxide synthesis by oxygen. Am J Physiol Heart Circ Physiol. 2003; 284(4):H1230–9. [PubMed: 12505879]

159. Tsai AG, Acero C, Nance PR, Cabrales P, Frangos JA, Buerk DG, et al. Elevated plasma viscosity in extreme hemodilution increases perivascular nitric oxide concentration and microvascular perfusion. Am J Physiol Heart Circ Physiol. 2005; 288(4):H1730–9. [PubMed: 15576432]

160. Mitchell D, Tyml K. Nitric oxide release in rat skeletal muscle capillary. Am J Physiol. 1996; 270(5 Pt 2):H1696–703. [PubMed: 8928876]

161. Grzelec-Mojzesowicz M, Sadowski J. Renal tissue NO and intrarenal haemodynamics during experimental variations of NO content in anaesthetised rats. J Physiol Pharmacol. 2007; 58(1): 149–63. [PubMed: 17440233]

162. Noiri E, Peresleni T, Miller F, Goligorsky MS. In vivo targeting of inducible NO synthase with oligodeoxynucleotides protects rat kidney against ischemia. J Clin Invest. 1996; 97(10):2377–83. [PubMed: 8636419]

163. Heyman SN, Karmeli F, Rachmilewitz D, Haj-Yehia A, Brezis M. Intrarenal nitric oxide monitoring with a Clark-type electrode: potential pitfalls. Kidney Int. 1997; 51(5):1619–23. [PubMed: 9150482]

164. Arregui B, Lopez B, Garcia Salom M, Valero F, Navarro C, Fenoy FJ. Acute renal hemodynamic effects of dimanganese decacarbonyl and cobalt protoporphyrin. Kidney Int. 2004; 65(2):564–74. [PubMed: 14717926]

165. Barbosa RM, Lourenco CF, Santos RM, Pomerleau F, Huettl P, Gerhardt GA, et al. In vivo real-time measurement of nitric oxide in anesthetized rat brain. Methods Enzymol. 2008; 441:351–67. [PubMed: 18554545]

166. Lourenco CF, Santos R, Barbosa RM, Gerhardt G, Cadenas E, Laranjinha J. In vivo modulation of nitric oxide concentration dynamics upon glutamatergic neuronal activation in the hippocampus. Hippocampus. 2011; 21:622–30. [PubMed: 20169537]

167. Ledo A, Barbosa R, Cadenas E, Laranjinha J. Dynamic and interacting profiles of *NO and O_2 in rat hippocampal slices. Free Radic Biol Med. 2010; 48(8):1044–50. [PubMed: 20100565]

168. Ledo A, Barbosa RM, Gerhardt GA, Cadenas E, Laranjinha J. Concentration dynamics of nitric oxide in rat hippocampal subregions evoked by stimulation of the NMDA glutamate receptor. Proc Natl Acad Sci U S A. 2005; 102(48):17483–8. [PubMed: 16293699]

169. Lowe G, Buerk DG, Ma J, Gelperin A. Tonic and stimulus-evoked nitric oxide production in the mouse olfactory bulb. Neuroscience. 2008; 153(3):842–50. [PubMed: 18407420]

170. Buerk DG, Ances BM, Greenberg JH, Detre JA. Temporal dynamics of brain tissue nitric oxide during functional forepaw stimulation in rats. Neuroimage. 2003; 18(1):1–9. [PubMed: 12507439]

171. Kashiwagi S, Izumi Y, Gohongi T, Demou ZN, Xu L, Huang PL, et al. NO mediates mural cell recruitment and vessel morphogenesis in murine melanomas and tissue-engineered blood vessels. J Clin Invest. 2005; 115(7):1816–37. [PubMed: 15951843]

172. Buerk DG, Riva CE. Vasomotion and spontaneous low-frequency oscillations in blood flow and nitric oxide in cat optic nerve head. Microvasc Res. 1998; 55(1):103–12. [PubMed: 9473413]

173. Palm F, Buerk DG, Carlsson PO, Hansell P, Liss P. Reduced nitric oxide concentration in the renal cortex of streptozotocin-induced diabetic rats: effects on renal oxygenation and microcirculation. Diabetes. 2005; 54(11):3282–7. [PubMed: 16249456]

174. Mason RP, Kubant R, Jacob RF, Malinski P, Huang X, Louka FR, et al. Loss of arterial and renal nitric oxide bioavailability in hypertensive rats with diabetes: effect of beta-blockers. Am J Hypertens. 2009; 22(11):1160–6. [PubMed: 19730416]

175. Malinski T, Bailey F, Zhang ZG, Chopp M. Nitric oxide measured by a porphyrinic microsensor in rat brain after transient middle cerebral artery occlusion. J Cereb Blood Flow Metab. 1993; 13(3):355–8. [PubMed: 8478395]
176. Zhang ZG, Chopp M, Bailey F, Malinski T. Nitric oxide changes in the rat brain after transient middle cerebral artery occlusion. J Neurol Sci. 1995; 128(1):22–7. [PubMed: 7536815]
177. Kidd GA, Dobrucki LW, Brovkovych V, Bohr DF, Malinski T. Nitric oxide deficiency contributes to large cerebral infarct size. Hypertension. 2000; 35(5):1111–8. [PubMed: 10818073]
178. Yang Y, Ke-Zhou L, Ning GM, Wang ML, Zheng XX. Dynamics of nitric oxide and peroxynitrite during global brain ischemia/reperfusion in rat hippocampus: NO-sensor measurement and modeling study. Neurochem Res. 2008; 33(1):73–80. [PubMed: 17674204]
179. Liu K, Li Q, Zhang L, Zheng X. The dynamic detection of NO during stroke and reperfusion in vivo. Brain Inj. 2009; 23(5):450–8. [PubMed: 19408167]
180. Demchenko IT, Boso AE, Whorton AR, Piantadosi CA. Nitric oxide production is enhanced in rat brain before oxygen-induced convulsions. Brain Res. 2001; 917(2):253–61. [PubMed: 11640911]
181. Thom SR, Bhopale V, Fisher D, Manevich Y, Huang PL, Buerk DG. Stimulation of nitric oxide synthase in cerebral cortex due to elevated partial pressures of oxygen: an oxidative stress response. J Neurobiol. 2002; 51(2):85–100. [PubMed: 11932951]
182. Demchenko IT, Ruehle A, Allen BW, Vann RD, Piantadosi CA. Phosphodiesterase-5 inhibitors oppose hyperoxic vasoconstriction and accelerate seizure development in rats exposed to hyperbaric oxygen. J Appl Physiol. 2009; 106(4):1234–42. [PubMed: 19179645]
183. Cleeter MW, Cooper JM, Darley-Usmar VM, Moncada S, Schapira AH. Reversible inhibition of cytochrome c oxidase, the terminal enzyme of the mitochondrial respiratory chain, by nitric oxide. Implications for neurodegenerative diseases. FEBS Lett. 1994; 345(1):50–4. [PubMed: 8194600]
184. Taylor CT, Moncada S. Nitric oxide, cytochrome C oxidase, and the cellular response to hypoxia. Arterioscler Thromb Vasc Biol. 2010; 30(4):643–7. [PubMed: 19713530]
185. Brown GC, Cooper CE. Nanomolar concentrations of nitric oxide reversibly inhibit synaptosomal respiration by competing with oxygen at cytochrome oxidase. FEBS Lett. 1994; 356(2-3):295–8. [PubMed: 7805858]
186. Schweizer M, Richter C. Nitric oxide potently and reversibly deenergizes mitochondria at low oxygen tension. Biochem Biophys Res Commun. 1994; 204(1):169–75. [PubMed: 7945356]
187. Koivisto A, Matthias A, Bronnikov G, Nedergaard J. Kinetics of the inhibition of mitochondrial respiration by NO. FEBS Lett. 1997; 417(1):75–80. [PubMed: 9395078]
188. Antunes F, Boveris A, Cadenas E. On the mechanism and biology of cytochrome oxidase inhibition by nitric oxide. Proc Natl Acad Sci U S A. Nov 30. 2004; 101(48):16774–9. [PubMed: 15546991]
189. Mason MG, Nicholls P, Wilson MT, Cooper CE. Nitric oxide inhibition of respiration involves both competitive (heme) and noncompetitive (copper) binding to cytochrome c oxidase. Proc Natl Acad Sci U S A. 2006; 103(3):708–13. [PubMed: 16407136]
190. Thomas DD, Liu X, Kantrow SP, Lancaster JR Jr. The biological lifetime of nitric oxide: implications for the perivascular dynamics of NO and O_2. Proc Natl Acad Sci U S A. 2001; 98(1):355–60. [PubMed: 11134509]
191. Lamkin-Kennard K, Jaron D, Buerk DG. Modeling the regulation of oxygen consumption by nitric oxide. Adv Exp Med Biol. 2003; 510:145–59. [PubMed: 12580419]
192. Shen W, Xu X, Ochoa M, Zhao G, Wolin MS, Hintze TH. Role of nitric oxide in the regulation of oxygen consumption in conscious dogs. Circ Res. 1994; 75(6):1086–95. [PubMed: 7525103]
193. Laycock SK, Vogel T, Forfia PR, Tuzman J, Xu X, Ochoa M, et al. Role of nitric oxide in the control of renal oxygen consumption and the regulation of chemical work in the kidney. Circ Res. 1998; 82(12):1263–71. [PubMed: 9648722]
194. Deng A, Miracle CM, Suarez JM, Lortie M, Satriano J, Thomson SC, et al. Oxygen consumption in the kidney: effects of nitric oxide synthase isoforms and angiotensin II. Kidney Int. 2005; 68(2):723–30. [PubMed: 16014049]

195. King CE, Melinyshyn MJ, Mewburn JD, Curtis SE, Winn MJ, Cain SM, et al. Canine hindlimb blood flow and O_2 uptake after inhibition of EDRF/NO synthesis. J Appl Physiol. 1994; 76(3): 1166–71. [PubMed: 7516323]

196. Sherman AJ, Davis CA 3rd, Klocke FJ, Harris KR, Srinivasan G, Yaacoub AS, et al. Blockade of nitric oxide synthesis reduces myocardial oxygen consumption in vivo. Circulation. 1997; 95(5): 1328–34. [PubMed: 9054867]

197. Kirkeboen KA, Naess PA, Offstad J, Ilebekk A. Effects of regional inhibition of nitric oxide synthesis in intact porcine hearts. Am J Physiol. 1994; 266(4 Pt 2):H1516–27. [PubMed: 8184929]

198. Williams JG, Ojaimi C, Qanud K, Zhang S, Xu X, Recchia FA, et al. Coronary nitric oxide production controls cardiac substrate metabolism during pregnancy in the dog. Am J Physiol Heart Circ Physiol. 2008; 294(6):H2516–23. [PubMed: 18424630]

199. Victor VM, Nunez C, D'Ocon P, Taylor CT, Esplugues JV, Moncada S. Regulation of oxygen distribution in tissues by endothelial nitric oxide. Circ Res. 2009; 104(10):1178–83. [PubMed: 19407240]

200. Cabrales P, Tsai AG, Frangos JA, Intaglietta M. Role of endothelial nitric oxide in microvascular oxygen delivery and consumption. Free Radic Biol Med. 2005; 39(9):1229–37. [PubMed: 16214038]

201. Shibata M, Ichioka S, Kamiya A. Estimating oxygen consumption rates of arteriolar walls under physiological conditions in rat skeletal muscle. Am J Physiol Heart Circ Physiol. 2005; 289(1):H295–300. [PubMed: 15665059]

202. Shibata M, Qin K, Ichioka S, Kamiya A. Vascular wall energetics in arterioles during nitric oxide-dependent and -independent vasodilation. J Appl Physiol. 2006; 100(6):1793–8. [PubMed: 16497835]

203. Shibata M, Ichioka S, Kamiya A. Nitric oxide modulates oxygen consumption by arteriolar walls in rat skeletal muscle. Am J Physiol Heart Circ Physiol. 2005; 289(6):H2673–9. [PubMed: 16040716]

204. Liu X, Srinivasan P, Collard E, Grajdeanu P, Lok K, Boyle SE, et al. Oxygen regulates the effective diffusion distance of nitric oxide in the aortic wall. Free Radic Biol Med. 2010; 48(4): 554–9. [PubMed: 19969071]

205. Wink DA, Darbyshire JF, Nims RW, Saavedra JE, Ford PC. Reactions of the bioregulatory agent nitric oxide in oxygenated aqueous media: determination of the kinetics for oxidation and nitrosation by intermediates generated in the NO/O_2 reaction. Chem Res Toxicol. 1993; 6(1):23–7. [PubMed: 8448345]

206. Lewis RS, Deen WM. Kinetics of the reaction of nitric oxide with oxygen in aqueous solutions. Chem Res Toxicol. 1994; 7(4):568–74. [PubMed: 7981422]

207. Halligan KE, Jourd'heuil FL, Jourd'heuil D. Cytoglobin is expressed in the vasculature and regulates cell respiration and proliferation via nitric oxide dioxygenation. J Biol Chem. 2009; 284(13):8539–47. [PubMed: 19147491]

208. Coffey MJ, Natarajan R, Chumley PH, Coles B, Thimmalapura PR, Nowell M, et al. Catalytic consumption of nitric oxide by 12/15- lipoxygenase: inhibition of monocyte soluble guanylate cyclase activation. Proc Natl Acad Sci U S A. 2001; 98(14):8006–11. [PubMed: 11427723]

209. O'Donnell VB, Taylor KB, Parthasarathy S, Kuhn H, Koesling D, Friebe A, et al. 15-Lipoxygenase catalytically consumes nitric oxide and impairs activation of guanylate cyclase. J Biol Chem. 1999; 274(29):20083–91. [PubMed: 10400618]

210. Eiserich JP, Baldus S, Brennan ML, Ma W, Zhang C, Tousson A, et al. Myeloperoxidase, a leukocyte-derived vascular NO oxidase. Science. 2002; 296(5577):2391–4. [PubMed: 12089442]

211. Azizi F, Kielbasa JE, Adeyiga AM, Maree RD, Frazier M, Yakubu M, et al. Rates of nitric oxide dissociation from hemoglobin. Free Radic Biol Med. 2005; 39(2):145–51. [PubMed: 15964506]

212. Shiva S, Wang X, Ringwood LA, Xu X, Yuditskaya S, Annavajjhala V, et al. Ceruloplasmin is a NO oxidase and nitrite synthase that determines endocrine NO homeostasis. Nat Chem Biol. 2006; 2(9):486–93. [PubMed: 16906150]

213. Crawford JH, Isbell TS, Huang Z, Shiva S, Chacko BK, Schechter AN, et al. Hypoxia, red blood cells, and nitrite regulate NO-dependent hypoxic vaso-dilation. Blood. 2006; 107(2):566–74. [PubMed: 16195332]

214. Diesen DL, Hess DT, Stamler JS. Hypoxic vasodilation by red blood cells: evidence for an s-nitrosothiol-based signal. Circ Res. 2008; 103(5):545–53. [PubMed: 18658051]

215. Isbell TS, Sun CW, Wu LC, Teng X, Vitturi DA, Branch BG, et al. SNO-hemoglobin is not essential for red blood cell-dependent hypoxic vasodilation. Nat Med. 2008; 14(7):773–7. [PubMed: 18516054]

216. Chen K, Pittman RN, Popel AS. Vascular smooth muscle NO exposure from intraerythrocytic SNOHb: a mathematical model. Antioxid Redox Signal. 2007; 9(8):1097–110. [PubMed: 17536957]

217. Bennett-Guerrero E, Veldman TH, Doctor A, Telen MJ, Ortel TL, Reid TS, et al. Evolution of adverse changes in stored RBCs. Proc Natl Acad Sci U S A. 2007; 104(43):17063–8. [PubMed: 17940021]

218. Reynolds JD, Ahearn GS, Angelo M, Zhang J, Cobb F, Stamler JS. S-nitrosohemoglobin deficiency: a mechanism for loss of physiological activity in banked blood. Proc Natl Acad Sci U S A. 2007; 104(43):17058–62. [PubMed: 17940022]

219. Chen LY, Mehta JL. Evidence for the presence of L-arginine-nitric oxide pathway in human red blood cells: relevance in the effects of red blood cells on platelet function. J Cardiovasc Pharmacol. 1998; 32(1):57–61. [PubMed: 9676721]

220. Kang ES, Ford K, Grokulsky G, Wang YB, Chiang TM, Acchiardo SR. Normal circulating adult human red blood cells contain inactive NOS proteins. J Lab Clin Med. 2000; 135(6):444–51. [PubMed: 10850643]

221. Kleinbongard P, Schulz R, Rassaf T, Lauer T, Dejam A, Jax T, et al. Red blood cells express a functional endothelial nitric oxide synthase. Blood. 2006; 107(7):2943–51. [PubMed: 16368881]

222. Ulker P, Sati L, Celik-Ozenci C, Meiselman HJ, Baskurt OK. Mechanical stimulation of nitric oxide synthesizing mechanisms in erythrocytes. Biorheology. 2009; 46(2):121–32. [PubMed: 19458415]

223. Gladwin MT, Grubina R, Doyle MP. The new chemical biology of nitrite reactions with hemoglobin: R-state catalysis, oxidative denitrosylation, and nitrite reductase/anhydrase. Acc Chem Res. 2009; 42(1):157–67. [PubMed: 18783254]

224. van Faassen EE, Bahrami S, Feelisch M, Hogg N, Kelm M, Kim-Shapiro DB, et al. Nitrite as regulator of hypoxic signaling in mammalian physiology. Med Res Rev. 2009; 29(5):683–741. [PubMed: 19219851]

225. Jensen FB, Rohde S. Comparative analysis of nitrite uptake and hemoglobin-nitrite reactions in erythrocytes: sorting out uptake mechanisms and oxygenation dependencies. Am J Physiol Regul Integr Comp Physiol. 2010; 298(4):R972–82. [PubMed: 20130222]

226. Dejam A, Hunter CJ, Pelletier MM, Hsu LL, Machado RF, Shiva S, et al. Erythrocytes are the major intravascular storage sites of nitrite in human blood. Blood. 2005; 106(2):734–9. [PubMed: 15774613]

227. Doyle MP, Pickering RA, DeWeert TM, Hoekstra JW, Pater D. Kinetics and mechanism of the oxidation of human deoxyhemoglobin by nitrites. J Biol Chem. 1981; 256(23):12393–8. [PubMed: 7298665]

228. Vitturi DA, Teng X, Toledo JC, Matalon S, Lancaster JR Jr. Patel RP. Regulation of nitrite transport in red blood cells by hemoglobin oxygen fractional saturation. Am J Physiol Heart Circ Physiol. 2009; 296(5):H1398–407. [PubMed: 19286940]

229. Gladwin MT, Kim-Shapiro DB. The functional nitrite reductase activity of the heme-globins. Blood. 2008; 112(7):2636–47. [PubMed: 18596228]

230. Chen K, Piknova B, Pittman RN, Schechter AN, Popel AS. Nitric oxide from nitrite reduction by hemoglobin in the plasma and erythrocytes. Nitric Oxide. 2008; 18(1):47–60. [PubMed: 17964300]

231. Feelisch M, Fernandez BO, Bryan NS, Garcia-Saura MF, Bauer S, Whitlock DR, et al. Tissue processing of nitrite in hypoxia: an intricate interplay of nitric oxide-generating and -scavenging systems. J Biol Chem. 2008; 283(49):33927–34. [PubMed: 18835812]

232. Li H, Cui H, Kundu TK, Alzawahra W, Zweier JL. Nitric oxide production from nitrite occurs primarily in tissues not in the blood: critical role of xanthine oxidase and aldehyde oxidase. J Biol Chem. 2008; 283(26):17855–63. [PubMed: 18424432]

233. Alzawahra WF, Talukder MA, Liu X, Samouilov A, Zweier JL. Heme proteins mediate the conversion of nitrite to nitric oxide in the vascular wall. Am J Physiol Heart Circ Physiol. 2008; 295(2):H499–508. [PubMed: 18539756]

234. Buerk DG, Barbee KA, Jaron D. Modeling O_2-dependent effects of nitrite reductase activity in blood and tissue on coupled NO and O_2 transport around arterioles. Adv Exp Med Biol. 2010; 701:271–6. [PubMed: 21445797]

235. Ellsworth ML, Forrester T, Ellis CG, Dietrich HH. The erythrocyte as a regulator of vascular tone. Am J Physiol. 1995; 269(6 Pt 2):H2155–61. [PubMed: 8594927]

236. Bergfeld GR, Forrester T. Release of ATP from human erythrocytes in response to a brief period of hypoxia and hypercapnia. Cardiovasc Res. 1992; 26(1):40–7. [PubMed: 1325292]

237. Sprague RS, Ellsworth ML, Stephenson AH, Lonigro AJ. ATP: the red blood cell link to NO and local control of the pulmonary circulation. Am J Physiol. 1996; 271(6 Pt 2):H2717–22. [PubMed: 8997335]

238. Olearczyk JJ, Stephenson AH, Lonigro AJ, Sprague RS. NO inhibits signal transduction pathway for ATP release from erythrocytes via its action on heterotrimeric G protein G_i. Am J Physiol Heart Circ Physiol. 2004; 287(2):H748–54. [PubMed: 15072952]

239. Garcia JI, Seabra AB, Kennedy R, English AM. Nitrite and nitroglycerin induce rapid release of the vasodilator ATP from erythrocytes: Relevance to the chemical physiology of local vasodilation. J Inorg Biochem. 2010; 104(3):289–96. [PubMed: 20074809]

240. Cao Z, Bell JB, Mohanty JG, Nagababu E, Rifkind JM. Nitrite enhances RBC hypoxic ATP synthesis and the release of ATP into the vasculature: a new mechanism for nitrite-induced vasodilation. Am J Physiol Heart Circ Physiol. 2009; 297(4):H1494–503. [PubMed: 19700624]

241. da Silva CG, Specht A, Wegiel B, Ferran C, Kaczmarek E. Mechanism of purinergic activation of endothelial nitric oxide synthase in endothelial cells. Circulation. 2009; 119(6):871–9. [PubMed: 19188511]

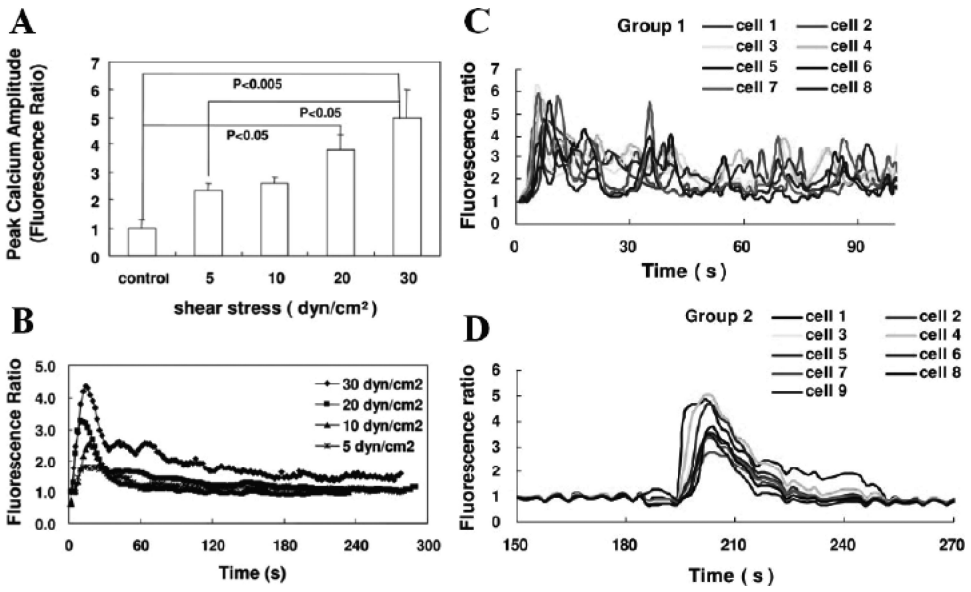

FIGURE 1.

Calcium fluorescence data from Hong et al.[22] obtained with bovine aortic endothelial cells (BAECs) (A, B) and rat adrenomedulary endothelial cells (ECs) derived from capillary endothelium (C, D). Synchronous Ca^{2+} responses with similar shear stress–dependent peak values were observed with BAECs, but heterogeneous Ca^{2+} responses were observed (C) with rat adrenomedulary ECs, although some cells had a synchronized response delayed in time after an increase in shear stress (D). Modified from Figs. 1 and 2 in Hong et al.[22], with permission from the American Journal of Physiology.

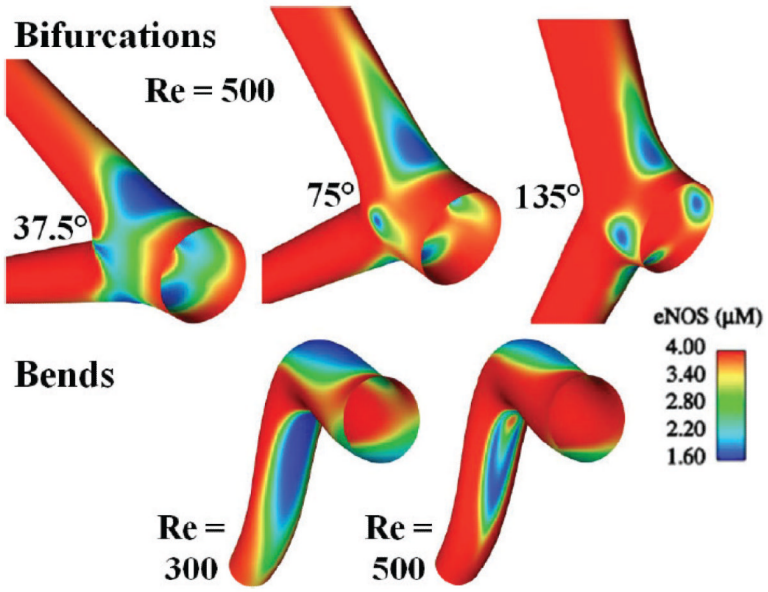

FIGURE 2.

Computer simulations conducted by Comerford et al.[49] for spatial distributions of endothelial nitric oxide synthase (eNOS) protein in vascular bifurcations and bends. Regions with low wall shear stress (WSS; calculated from a fluid dynamics model) are associated with low eNOS expression and based on a functional relationship determined for eNOS with WSS from experimental studies by Cheng et al.[48,58] Modified from Figs. 7 and 11 in Comerford et al.[49], with permission from the Journal of Biomechanical Engineering.

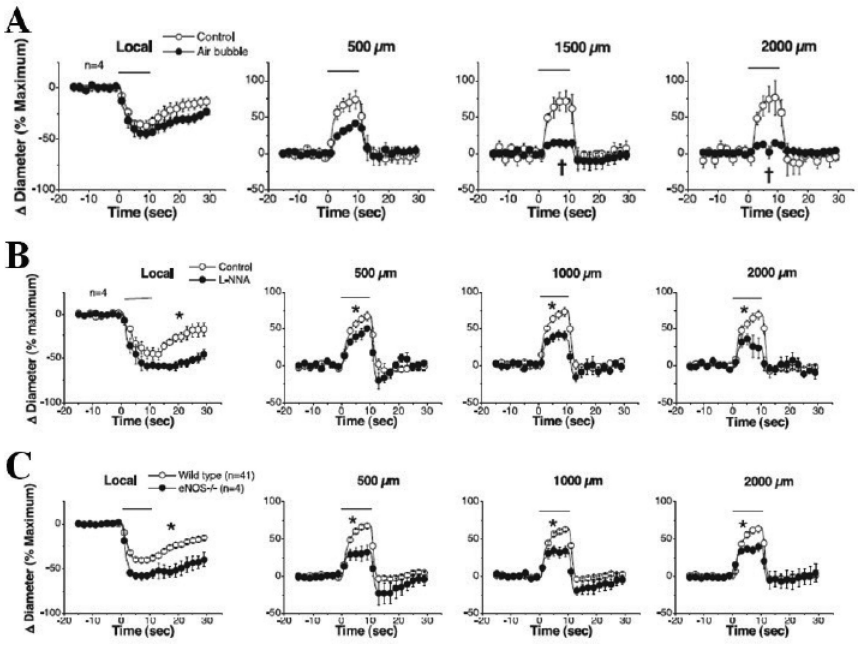

FIGURE 3.

In vivo studies of endothelium-dependent propagated vascular responses to local electrical stimulation in the mouse cremaster microcirculation by Figueroa et al.[71] Removal of endothelium at the simulation site by air embolism greatly attenuates downstream responses (A); an inhibitor of nitric oxide (NO) production partially attenuates propagated responses (B); and propagated responses are smaller in endothelial NO synthase knockout mice compared with wild-type mice (C). Modified from Figs. 2 and 7 in Figueroa et al.[71], with permission from the American Journal of Physiology.

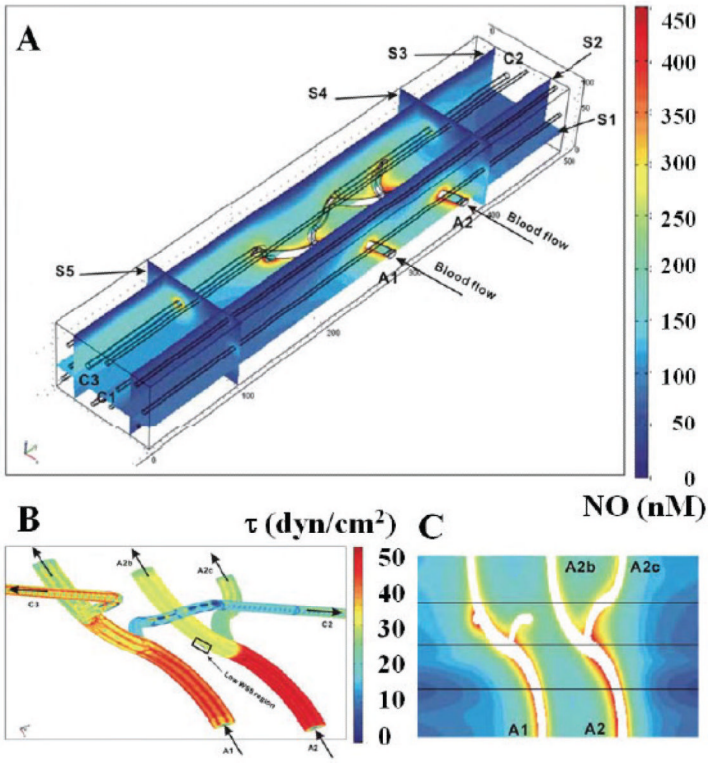

FIGURE 4.

Computational model of 3-dimensional microcirculatory network by Chen[117] predicting nitric oxide (NO) distributions (A) with different blood flow rates. Distribution of wall shear stress in 2 branching arterioles (B) and redistribution of red blood cells with branching have an impact on the NO distribution (C) around these branches. Reprinted from Chen.[117]

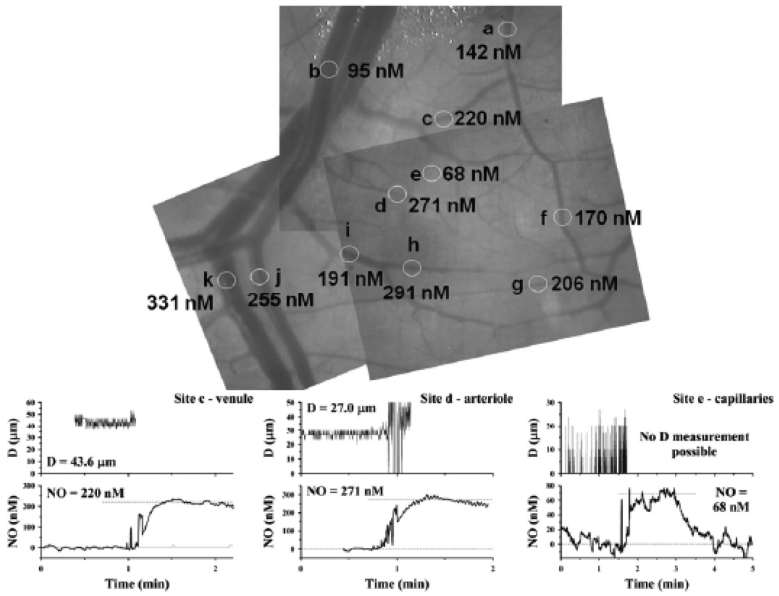

FIGURE 5.

Mapping of perivascular nitric oxide (NO) in superfused rat mesentery and small intestine conducted in our laboratory (unpublished) using Nafion-coated recessed NO microelectrodes (top panel). Examples of experimental vessel diameter measurements and NO measurements also are shown (bottom graphs). For venule and arteriole measurements, the NO microelectrode initially was positioned far from the vessel (zero reading), then moved to touch the outer surface of the vessel gently (perivascular NO value). The microelectrode image interfered with video diameter measurements when it was near the vessel (for clarity, the diameter signal is removed just before the tip touches the vessel). For the capillary-perfused site, the NO microelectrode was initially far from the tissue surface, then was moved to the surface and back out into the superfusion bath. The NO microelectrode current was converted to concentration based on calibrations at known NO concentrations.

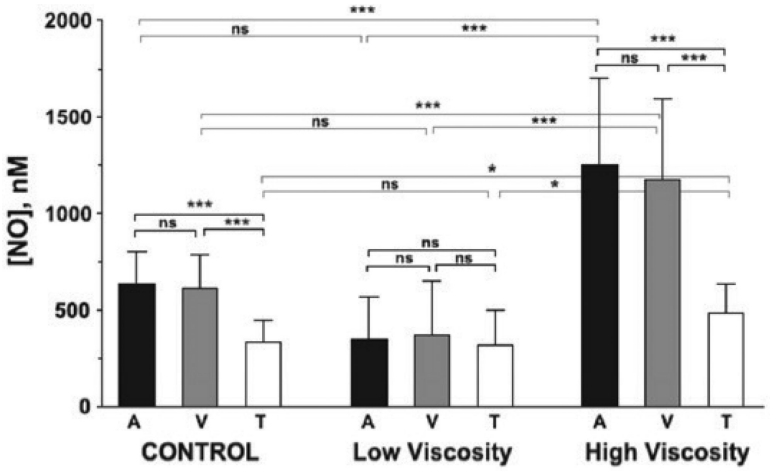

FIGURE 6.

In vivo study by Tsai et al.[159] using nitric oxide (NO) microelectrodes to measure perivascular and tissue (T) NO in the dorsal skin chamber of unanesthetized hamsters for control animals and animals receiving isovolemic hemodilution with either low- or high-viscosity solutions. *P < 0.05. **P < 0.01. ***P < 0.001. A, arteriole; NS, not significant; V, venule. Modified from Fig. 5 in Tsai et al.[159], with permission from the American Journal of Physiology.

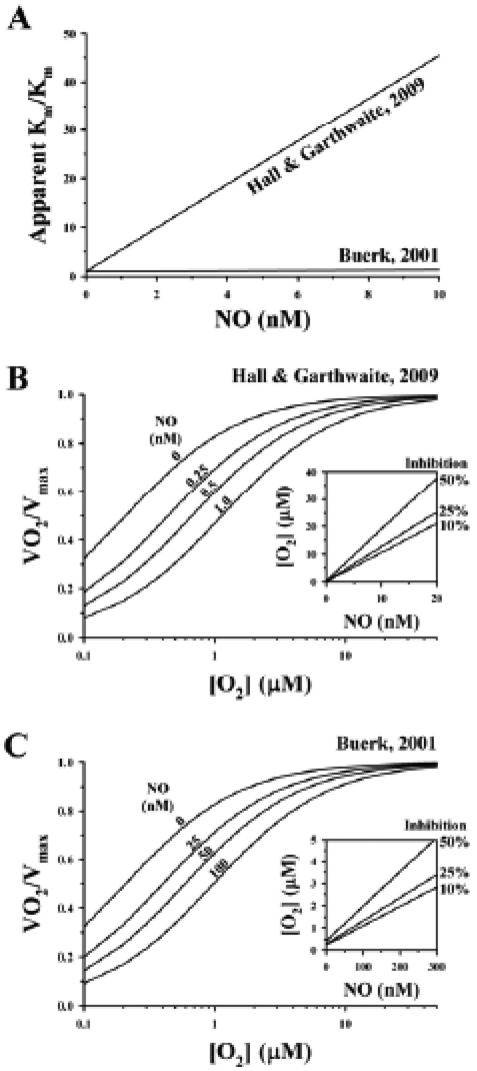

FIGURE 7.

Differences in effects of nitric oxide (NO) on inhibition of O_2 consumption as modeled by Buerk[88] and Hall and Garthwaite.[6] The model by Hall and Garthwaite[6] has a stronger dependence of apparent K_m on NO (A), with greater inhibition of O_2 consumption by NO (B) than that predicted from model by Buerk[88] (C).

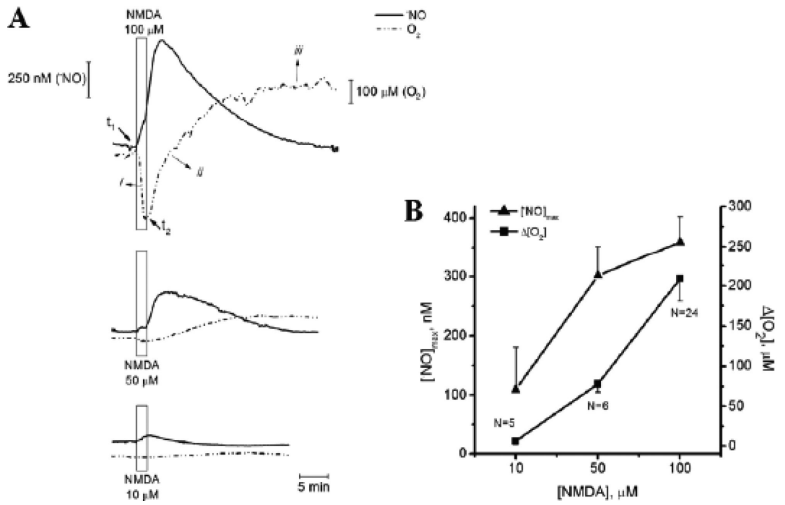

FIGURE 8.

In vitro measurements by Ledo et al.[167] of changes in nitric oxide (NO) and tissue O_2 in rat hippocampus slice following pressure injection of different concentrations of N-methyl-D-aspartic acid (A) provides evidence for inhibition of O_2 consumption by NO because tissue O_2 increases with higher NO (B). Modified from Figs. 1 and 2 in Ledo et al.[167],with permission from Free Radical Biology and Medicine.